ISSN 0742-0463, Journal of Volcanology and Seismology, 2008, Vol. 2, No. 4, pp. 228–247. © Pleiades Publishing, Ltd., 2008.
Original Russian Text © E.N. Grib, A.B. Perepelov, 2008, published in Vulkanologiya i Seismologiya, 2008, No. 4, pp. 14–35.

Olivine Basalts at the Karymskii Volcanic Center: Mineralogy, Petrogenesis, and Magma Sources

E. N. Grib[a] and A. B. Perepelov[b]

[a] *Institute of Volcanology and Seismology, Far East Division, Russian Academy of Sciences, Petropavlovsk-Kamchatskii, 683006 Russia*

[b] *Vinogradov Institute of Geochemistry, Siberian Branch, Russian Academy of Sciences, Irkutsk, 664033 Russia*

Received December 20, 2007

Abstract—The olivine basalts of the Karymskii Volcanic Center (KVC) can be traced during the history of the area from the Lower Pleistocene until recently (the 1996 events); they are typical low- and moderate-potassium tholeiite basalts of the geochemical island-arc type. We have investigated the compositions of phenocryst minerals represented by plagioclase, olivine, clinopyroxene, as well as solid-phase inclusions of spinel in olivine, and more rarely in anorthite. The evolutionary trends of the rock-forming minerals provide evidence of the comagmaticity of these basalts, and thus of a long-lived intermediate magma chamber in the interior of the structure. The activity of this chamber is related to periodic transport of high temperature basalt melts to the surface. The geochemistry of the basalts is controlled by their origin at the same depleted magma source close to N-MORB, by successive crystallization of the primary melt, and by restricted mixing with magma components that are crystallizing at different depths. It is hypothesized that the solid-phase inclusions of high alumina spinel (hercynite?) found in olivine (and anorthite) of the basalts in the KVC north sector are of relict origin.

DOI: 10.1134/S0742046308040027

INTRODUCTION

The Karymskii Volcanic Center (KVC) is situated in the central part of the Eastern Volcanic Belt of Kamchatka, and is a major volcano-tectonic feature. It began to form in the Pliocene (N_2) and has continued its evolution for 2 to 3 million years [6, 9, 10, 11, 18]. Several centers of basaltic volcanism formed within the KVC during Quaternary time (Fig. 1), the larger of these being in the north (Stena and Sobolinyi volcanoes) and in the south (Ditmara Volcano). The KVC was structurally rearranged in the beginning of the Middle Pleistocene (Q_2). Explosive eruptions discharged great amounts of pumice and ignimbrite (andesite–dacite, dacite, and rhyodacite in composition), producing the Stena–Sobolinyi double caldera in the north and the Polovinka caldera in the south. These calderas played a decisive role in dividing the KVC into two sectors, the Semyachik and the Akademicheskii [6] or the Northern and the Southern [9]. The subsequent evolution of each of these sectors has been self-contained. The Odnobokii, Belyankina, and Proto-Semyachik stratovolcanoes formed within the calderas, subsequently going through the same phases of caldera generation with volcanoes within them. In the beginning of the Upper Pleistocene (Q_3), a new center of volcanic activity formed in the central part of the feature; this center began its evolution from the pre-caldera Proto-Karymskii stratovolcano,, which generated the Karymskii caldera by a powerful explosive eruption in 7700 BP, which discharged pyroclastic pumice material [6]. Karymskii Volcano proper is situated within that caldera and is actively evolving even today, producing lavas of homogeneous andesite composition.

An unusual natural phenomenon occurred in the Karymskii Volcanic Center on January 1, 1996. That event consisted in a simultaneous subaerial eruption discharging basaltic tephra in the northern part of Lake Karymskii, which fills the Akademii Nauk caldera, and andesite lava from a new vent on Karymskii Volcano. These eruptions were preceded by a large (M = 6.9) earthquake beneath the Karymskii Volcanic Center [20]. The 1996 ejecta in Lake Karymskii consist of high-alumina tholeiitic low- and moderate-potassium basalts with a Pl–Ol–Cpx phenocryst association. A study of sections in the north shore of the lake revealed and dated layers of Holocene basaltic tephra that were obviously formed by events similar to the 1996 one [4]. They are also characterized by a Pl–Ol–Cpx phenocryst association. It should be noted that similar mineral associations are also typical of pre-caldera basalts discharged by Stena (the northern sector) and Ditmara (the southern sector) volcanoes, while all the later intracaldera volcanic edifices in the KVC, except for the volcanoes of the Malyi Semyachik group [18], are composed of calc-alkalic Opx–Cpx basalts. Olivine was also detected in the basalts of Odnobokii Volcano, but its association with anorthite belongs to disintegrated fragments of allivalite inclusions.

This paper reports results from detailed mineralogic, petrographic, and geochemical investigations of different-aged olivine basalts in the Karymskii Volcanic Center in order to discover the degree of their genetic

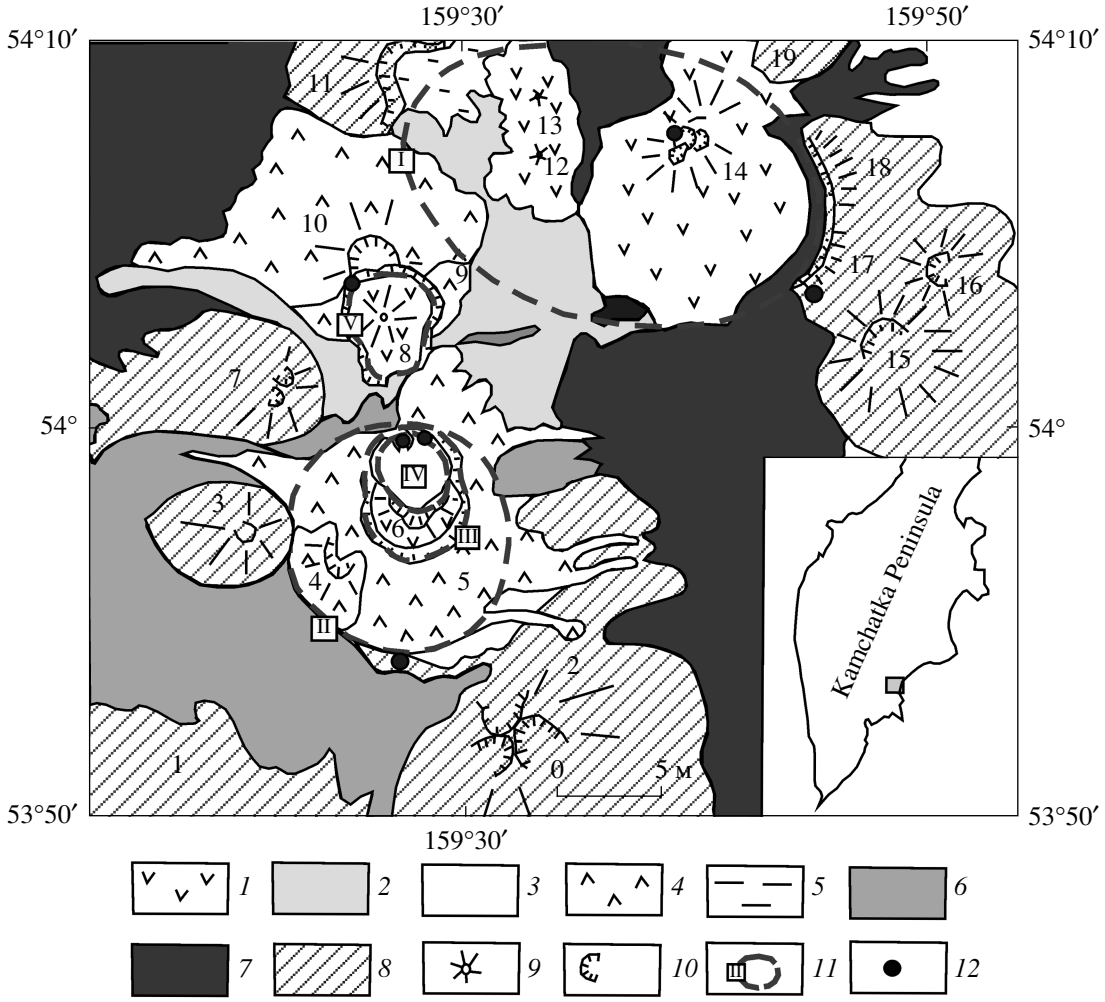

Fig. 1. A schematic geological map of the Karymskii Volcanic Center. The base map by V.L. Leonov with additions by the present authors. (*1*) a complex of lavas and pyroclastics of basaltic, basaltic andesite, and dacitic compositions in the Upper Pleistocene/Holocene (Q_3^4) volcanic edifices, (*2*) pumice tuffs of dacitic and rhyodacitic compositions related to the Karymskii caldera (Q), (*3*) pumice tuffs of dacitic and rhyodacitic compositions related to the Uzon–Geyser depression (($Q_{3–4}$); *4*), (*4*) a complex of lavas and pyroclastics of basaltic, basaltic andesite, and andesitic compositions in the Upper Pleistocene (Q_3) volcanic edifices, (*5*) a complex of intracaldera, volcanogenic–sedimentary, and lacustrine deposits (Q_3^1), (*6*) cinder, ignimbrites, and pumice tuffs of andesitic, dacitic, and rhyodacitic compositions related to the Polovinka caldera (Q_2^3), (*7*) ignimbrites of andesitic, dacite and rhyodacite compositions related to the Stena–Sobolinyi calderas, (*8*) lava, pyroclastics, and volcanogenic–sedimentary deposits in volcanic edifices formed during the pre-caldera phase (N_2–Q_1); (*9*) volcanoes: 1 Zhupanovskie Vostryaki, 2 Ditmara, 3 Krainii, 4 Belyankina, 5 Odnobokii, 6 Akademii Nauk, 7 Razlatyi, 8 Karymskii, 9 Proto-Karymskii, 10 Dvor, 11 Sobolinyi, 12 Sukhoi, 13 Stupenchatyi Bastion, 14 Malyi Semyachik, 15 Pribrezhnyi Yuzhnyi, 16 Pribrezhnyi Severnyi, 17 Stena, 18 Massivnyi, 19 Berezovyi; (*10*) erosion cirques, volcanic craters, calderas, (*11*) calderas: I double Stena–Sobolinyi calderas, II Polovinka, III Odnobokii, IV Akademii Nauk, V Karymskii; (*12*) sampling sites of olivine basalts. The square in the inset shows the area of study.

affinity and to estimate a possible composition of the source of primary melts for these basalts.

THE METHOD OF STUDY

The mineral composition in the KVC basalts was determined in isolated polished sections using monomineral fractions. The analysis of minerals was carried out using a Camebax-244 electron microanalyzer equipped with a Kevex energy-dispersion spectrometer at the Institute of Volcanology and Seismology of the Far East Division, Russ. Acad. Sci. (IVS FED RAS). The accelerating voltage was 20 kV and the current 40 nA. The number of analyses was 50 to 150 for each mineral investigated.

The bulk silicate chemical analyses of the basalts were carried out at the Central Chemical Laboratory of the IVS FED RAS using techniques of "wet" chemistry,

except for Na_2O and K_2O, which were determined by flame photometry. The concentrations of rare and rare-earth elements were determined by mass spectrometry (ICP-MS) at the Vernadsky Institute of Geochemistry of the Siberian Branch of the Russian Academy of Science.

THE TYPES AND PETROGRAPHY OF BASALTS

The olivine basalts are the most abundant in the north of the Karymskii Volcanic Center, in sections of the Malyi Semyachik volcanic massif [18]. The massif includes the Pliocene–Lower Quaternary pre-caldera Stena volcano, which was nearly destroyed by a later caldera-generating eruption, the intracaldera Proto-Semyachik volcano, and three Holocene volcanic edifices on Malyi Semyachik Volcano. All these volcanic edifices at the base of the sections are composed of high magnesia (8–11 wt % of MgO) low-potassium basalts involving abundant phenocrysts of Ol (8, more rarely 10–12 vol %), Cpx, and variable amounts of Pl. The phenocryst percentage in the lavas reaches 35–45 vol %. Higher in the section, magnesia basalts are gradually replaced with moderate-magnesia varieties (6–8 wt % of MgO), and still higher by leucocratic basalts. The phenocrysts of the latter are mostly composed of plagioclase with small amounts of late Ol and of still rarer Cpx. The amount of phenocrysts in lavas of leucocratic basalts reaches 30–40 vol %, this figure becoming as high as 50 vol % in sill-like bodies and dikes. The Malyi Semyachik basalts have porphyric and seriate porphyric textures, the groundmass texture being intersertal, microdolerite, pilotaxitic, and more rarely hyalopilitic. The larger (up to 2–4 mm) Ol phenocrysts are commonly idiomorphic or form growths of several grains, and frequently contain poikilitic inclusions of Pl and Cpx. The smaller (0.8–1 mm) Ol crystals form growths with Cpx and Pl.

The basalts of Ditmara Volcano have smaller phenocrysts (0.8–1.5 mm) and moderate degrees of crystallinity (25–35 vol %). Overall, the Ditmara sections are dominated by leucocratic basalt lavas, while magnesia varieties are smaller in volume and contain 7–8 wt % of MgO.

Sections in the north shore of Lake Karymskii contain Holocene olivine basalts identified at different hypsometric levels in the structure of terrace remnants. All of these are composed of volcanic tephra in the form of bombs, cinder, lapilli, and sand. The similarities between the basaltic material of the pyroclastic sections and the ejecta of the 1996 eruption suggest a similar mode of generation for them. The earliest Upper Pleistocene–Holocene (Q_3–Q_4) tephra layers of basic composition are found among the agglomerate pumice tuffs in the Odnobokii caldera and in the remnants of a high (abs. alt. 700 m) lacustrine terrace [9]. The tephra material consists of basaltic andesites and basalts involving small amounts (15–20 vol %) of a crystalline phase, which was found to contain ferrous olivine (Fo 70.7–72.9), clinopyroxene, and rare orthopyroxene. The northeast shore of the lake has a low three-meter lacustrine terrace that was hit by tsunami waves during the 1996 event. The terrace is underlain by a layer of bomb cinder consisting of agglomerate-grained basalt as thick as 1 m. Some denser basalt fragments 15–20 cm in size are found higher in the section in sand–clayey lacustrine deposits. The cinder layer has by now been nearly washed away. The eruption that discharged the cinder bombs found in the layer is dated 4800 BP [4]. The basalt texture is porphyric and glomerophyric; the phenocrysts make up no more than 20 vol %. Apart from plagioclase (up to 15% of rock volume), the phenocrysts were found to contain Ol and Cpx (3–5 vol %). Macroscopically, the olivine divides into a more ferrous, intensively yellowish type and a magnesia type in the form of light-colored, rounded grains containing a great amount of small solid-phase spinellid inclusions. The olivine phenocrysts form growths with plagioclase subphenocrysts in the margins, with the growths being as large as 2–3 mm. The cinder basalt in the terrace deposits have a moderately magnesia composition (6–7 wt % of MgO).

The basalts discharged by the 1996 eruption, which formed the Novogodnii Peninsula near the north shore of the lake, are black porous and glassy varieties containing great amounts of plagioclase phenocrysts (25–27 vol %); olivine and clinopyroxene are found in variable amounts, from 5 to 7 vol %. The concentration of MgO in the rocks is 5–6 wt %.

The lavas consisting of black, poorly porous glassy basalts (sample k10-05) found at the base of the northwest wall of the Karymskii caldera may also be classified as olivine-bearing. The glassy, fresh habit of these basalts and the small area of the exposures suggest that these basalts are from a dike, probably of Holocene age. Overall, the caldera walls are the base of the Proto-Karymskii volcano and are mostly composed of subaphyric andesites. The basalts at the base of the northwest caldera wall are found to contain great amounts (20–25 vol %) of plagioclase phenocrysts of tabular shape as large as 3–5 mm in size; they are immersed in a glassy mass, while Ol (1–2 vol %) is a later mineral, found in the groundmass and among plagioclase phenocrysts where its size does not exceed 0.4–0.6 mm. Clinopyroxene is found as isolated grains of 0.6 mm at most. The basalts are high in Al_2O_3 (18.9 wt %) and low in MgO (4.3 wt %).

The groundmass of the basalts discharged by explosive eruptions and the dikes have hyalopilitic texture and contains microlites of plagioclase, subcalcic augite, pigeonite, magnetite, and more rarely, olivine.

The basalts due to explosive eruptions and the dikes at the base of the northwest wall of the Karymskii caldera are assigned indices in what follows: 4800, 1996, and k10-05.

THE COMPOSITION OF BASALTIC PHENOCRYSTS

Plagioclase is dominant in all basalt types, except their varieties of higher magnesia content for the Stena–Malyi Semyachik massif. The amount of Pl varies within 15–25 vol % in magnesia varieties and to as much as 35–40 vol % in leucocratic varieties. Among the plagioclases one notes a phase of large, tabular-shaped, compositionally homogeneous phenocrysts (2–4 mm), mostly of anorthite composition (An 89–96) (Fig. 2, Table 1). There is another set consisting of smaller phenocrysts (0.8–2 mm) of bytownite–anorthite composition (An 87–91). These are elongate tabular in shape, are usually corroded, and saturated with partially crystallized melt and solid-phase inclusions. The phenocrysts most commonly exhibit normal zonality, with the composition in the marginal zones of crystals varying to An 75–65. The diagrams in Fig. 2 demonstrate that the first type of plagioclase phenocrysts dominates the basalts of the northern volcanoes and the dike in the wall of the Karymskii caldera.

Olivine is the dominant dark colored phenocryst mineral in magnesia basalts for Stena and Malyi Semyachik volcanoes. The Ol phenocrysts may be as large as 4-5 mm and make up to 5–7, and more rarely 10%, of the entire rock volume. Most crystals are red-brown in color, especially in lavas of the pre-caldera Stena volcano. Olivine contains rare, partially crystallized melt inclusions and a solid-phase, viz., solid versus solid-phase inclusions of spinel, plagioclase, and (to a lesser extent) clinopyroxene. The olivine phenocrysts are usually zonal. The olivine crystal nucleii are occasionally corroded, their composition is fairly homogeneous (Fo 75–82), the iron content being much higher in the marginal zones, Fo 58–65, more rarely 70 (Fig. 3, Table 2). The olivine in the basalt forming the dike in the Karymskii caldera wall has a similar composition.

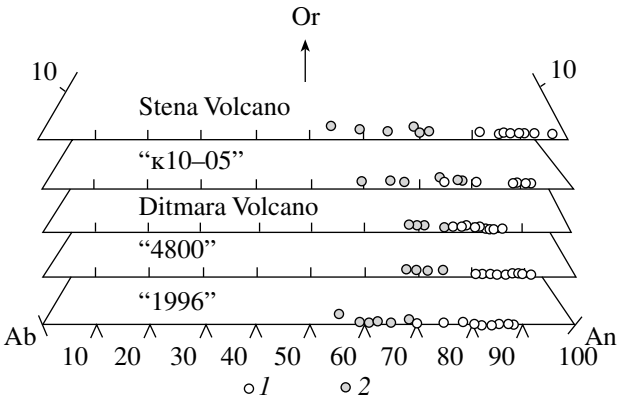

Fig. 2. The Ab–Or–An relationship in plagioclases of olivine basalts in the Karymskii Volcanic Center: (*1*) phenocryst nucleii, (*2*) margins.

The olivine in the phenocrysts found in the moderate-magnesia basalts of Ditmara Volcano and in the basaltic tephra from sections in the northern shore of Lake Karymskii is peculiar in that the compositions are bimodal. In the lavas of Ditmara Volcano one notes a generation of relatively ferruginous olivine phenocrysts (Fo 76–81) and a generation of dominant olivine with a higher content of magnesia (Fo 82–87). The basaltic tephra 4800 has a set of magnesia olivine (Fo 85–89) that is even more pronounced (Fig. 3). One also notes growths of olivine grains whose magnesia nucleii are surrounded by ferriferous margins. Plagioclase is crystallized at the periphery of such growths. Spinel grains as large as 70–100 μm are found at the center of the growths. It should be noted that the low-silica andesites and basaltic andesites found in the lava flows on the Holocene monogenetic Lagernyi cone north of Lake Karymskii contain olivine that is compositionally sim-

Table 1. Representative compositions of plagioclase phenocrysts (wt %) from basalts of the Karymskii Volcanic Center

Components	1c	2 mar	3 c	4 mar	5 c	6 mar	7 c	8 mar	9 c	10 mar	11 c	12 mar
SiO_2	44.83	50.87	45.17	47.34	46.09	49.46	47.68	47.92	45.09	45.51	45.63	51.06
Al_2O_3	33.39	30.67	33.38	33.38	36.18	33.39	33.34	33.00	34.74	34.45	34.67	30.28
FeO*	0.64	1.29	0.60	0.71	0.42	0.78	0.80	0.85	0.77	0.85	0.33	0.83
CaO	18.68	14.27	17.75	16.70	17.77	14.96	17.11	16.51	18.15	17.59	18.51	14.43
Na_2O	0.67	3.00	1.12	1.57	0.96	2.30	1.99	2.29	1.31	1.44	1.35	3.52
K_2O	0.02	0.16	0.04	0.05	0.02	0.04	0.08	0.07	0.01	0.04	0.06	0.24
Total	98.29	100.26	98.16	99.80	101.54	101.10	101.0	100.64	100.07	99.88	100.55	100.36
Or	0.10	1.08	0.24	0.03	0.15	0.25	0.43	0.42	0.06	0.21	0.35	1.34
Ab	6.08	27.24	10.25	14.48	8.86	21.75	17.32	19.98	11.53	12.90	11.58	30.18
An	93.82	70.68	89.51	85.22	90.99	78.00	82.25	79.60	88.41	86.89	88.07	68.48

Note: 1–4 Stena Volcano (sample S-564, O.B. Selyangin's collection); 5–6 dike of Proto-Karymskii Volcano (sample k10-05); 7–8 Ditmara Volcano (sample 21-99l, V.L. Leonov's collection), 9–10 4800 tephra (sample k6-06); 11–12 1996 tephra (sample k17-96). Here and below, mineral phases: c center, int intermediate zone, mar crystal margin; Or orthoclase, Ab albite and An anorthite minals of plagioclase, %. FeO*: here and below all Fe's are in the form FeO.

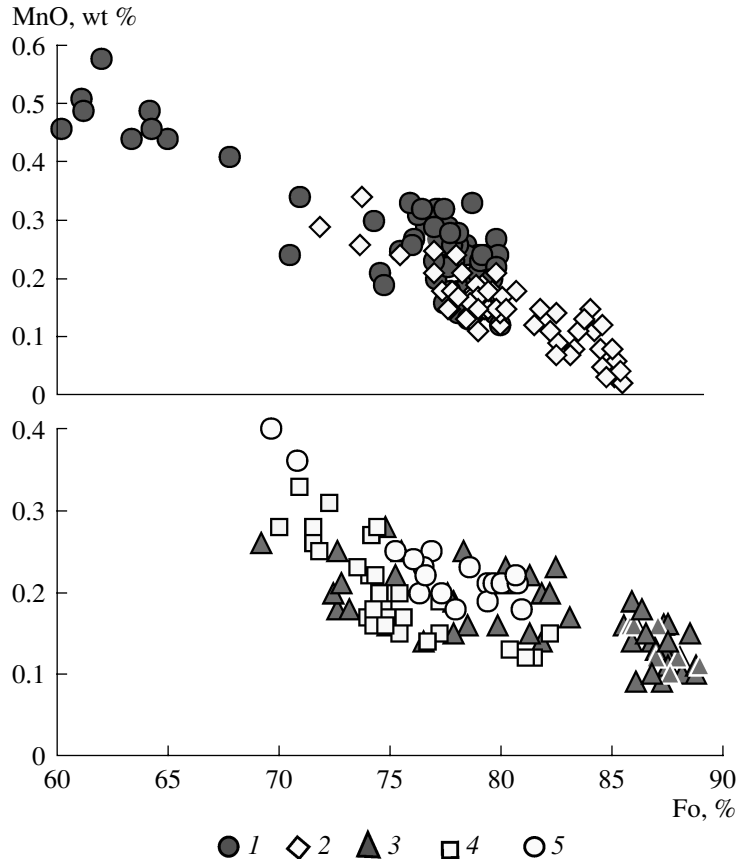

Fig. 3. Relationship of forsterite minal (Fo) and MnO in olivines of olivine-bearing basalts of the Karymskii Volcanic Center: (*1*) Stena and Malyi Semyachik volcanoes, lavas, (*2*) Ditmara Volcano, lavas, (*3*) 4800 basalts, tephra, (*4*) 1996 basalts, tephra, (*5*) dike in the northwest wall of the Karymskii caldera.

ilar to that in the 4800 basalts. The olivine in the 1996 tephra has Fo 73–83. Less ferriferrous compositions for the marginal zones of olivine phenocrysts discharged by Holocene explosive eruptions (Fig. 3) can be explained by the fact that the mineral stopped crystallizing owing to rapid cinder chilling during eruptions, with the explanation for Ditmara Volcano involving the rapid cooling of thin lava flows. With increasing iron content, the amount of MnO in basalt olivine is bound to do so too.

Clinopyroxene is present among phenocrysts in variable amounts, from 3–5 vol % in the Early Pleistocene pre-caldera basalts to 2–3 vol % in the Holocene ones. The Cpx phenocrysts have sizes of 0.8 to 1.5 mm. The Cpx crystals in the Stena lavas may be as large as 2.5 mm, while clinopyroxene is rarely found in the k10-05 basalts and its size does not exceed 0.5–0.6 mm. The crystals are frequently zonal, involve ferriferous or magnesia nucleii and a thin oscillating zonality in the marginal zone. The compositions vary between diopside and augite (Fig. 4a). The magnesia content of the clinopyroxenes varies within a wide range ($Mg^{\#}$ 71.3–86), but each object has its own relationship of phenocryst content to that quantity (Fig. 4b, Table 3). For example, the pre-caldera basalts of Stena Volcano (which have the highest magnesia content) contain the clinopyroxenes with the lowest magnesia content, viz., augites ($Mg^{\#}$ 72–80, $En_{40–46}$ $Wo_{39–46}$ $Fs_{10–16}$). The Ditmara lavas have a greater amount of magnesia-rich Cpx ($Mg^{\#}$ 75–84). The varieties with the highest content of magnesia were noted in basalts of the 4800 Holocene tephra; these are diopside and salite diopside ($Mg^{\#}$ 78–86, $En_{45–47}Wo_{45–48}$ $Fs_{7–11}$). The basalts discharged by the 1996 eruption are dominated by augite, while diopside is only found in nucleii of subphenocrysts [7]. The phenocrysts of different-aged basalts found in the Karymskii Volcanic Center as displayed in the $Mg^{\#}$ vs. oxide diagram exhibit consistent trends (Fig. 4b). As the content of magnesia decreases, so does that of CaO_2 and Cr_2O_3, while the concentrations of TiO_2 and Al_2O_3 slightly increase, with the increase being more noticeable for Na_2O; the most significant increase is observed for the Cpx from the 1996 basalts. One also notes an increased titanium content in the phenocrysts in the Ditmara basalts and an almost complete absence of Cr_2O_3 in the Cpx of the Stena lavas. The 4800 clinopyroxenes (with the highest content of magnesia) have the highest concentrations of CaO (22–23 wt %) and Cr_2O_3 (0.2–0.9 wt %).

Table 2. Representative compositions of olivine phenocrysts (wt %) from basalts of the Karymskii Volcanic Center

Components	1 c	2 int	3 mar	4 c	5 c	6 c	7 c	8 mar	9 c	10 c	11 c	12 c	13 c	14 mar
SiO_2	40.06	38.30	37.01	39.29	40.08	38.91	38.56	38.70	39.38	38.99	38.73	42.10	38.31	38.84
FeO^*	21.46	20.44	30.16	18.36	18.64	23.37	20.02	18.34	13.21	15.32	20.75	10.62	23.91	22.57
MgO	39.27	41.37	32.08	41.59	41.74	37.44	40.14	42.41	46.40	44.51	39.73	47.12	38.11	38.72
CaO	0.16	0.17	0.18	0.16	0.14	0.20	0.16	0.17	0.22	0.18	0.17	0.14	0.00	0.00
MnO	0.27	0.28	0.46	0.21	0.21	0.32	0.15	0.14	0.04	0.07	0.10	0.10	0.17	0.20
Total	101.22	100.56	99.89	99.61	100.81	100.24	99.03	99.76	99.25	99.07	99.48	100.08	100.5	100.33
Fo	76.5	78.3	65.1	80.2	80.0	74.1	78.1	80.5	86.2	83.8	77.3	88.8	74.0	75.4

Note: 1–4 Stena Volcano (sample S-564, O.B. Selyangin's collection); 5–6 dike in the wall of the Karymskii caldera (sample k10-05); 6 subphenocryst; 7–10 Ditmara Volcano (sample 21-99l, V.L. Leonov's collection); 10 subphenocryst; 11–12 480 tephra (sample k6-06); 13–14 1996 tephra (sample k17-96); Fo forsterite minal of olivine, %. For the other legend see Table 1.

Table 3. Representative compositions of clinopyroxene phenocrysts (wt %) from basalts of the Karymskii Volcanic Center

Components	1 c	2 int	3 mar	4 c	5 mar	6 c	7 mar	8 c	9 c	10 mar	11 c	12 int	13 mar
SiO_2	51.34	52.05	50.56	52.56	50.24	51.53	50.17	52.29	53.48	51.52	52.33	51.26	50.75
TiO_2	0.47	0.32	0.74	0.50	0.78	0.41	0.65	0.20	0.08	0.33	0.37	0.56	0.60
Al_2O_3	3.20	2.35	3.92	3.31	5.26	2.21	3.51	2.73	1.98	2.26	2.22	3.16	3.03
FeO^*	9.60	7.77	11.06	7.74	8.89	5.92	7.97	4.51	5.02	8.84	9.27	7.64	10.06
Cr_2O_3	0.00	0.09	0.00	0.03	0.00	0.29	0.21	0.92	0.22	0.00	0.00	0.05	0.00
MgO	14.58	15.70	13.22	16.03	14.33	17.04	15.65	15.45	16.84	15.43	15.56	14.68	14.03
CaO	20.23	20.53	19.81	18.46	18.53	21.09	20.36	22.79	22.66	21.33	19.38	20.84	19.46
Na2O	0.39	0.15	0.20	0.44	0.37	0.04	0.08	0.18	0.05	0.18	0.34	0.41	0.31
MnO	0.18	0.04	0.14	0.10	0.11	0.03	0.03	0.09	0.05	0.17	0.05	0.05	0.11
Total	99.99	99.00	99.65	99.17	98.51	98.56	98.63	99.16	100.24	100.06	99.52	98.55	99.35
$Mg^{\#}$	73.0	78.3	68.0	78.7	74.2	83.6	77.8	85.9	85.68	75.7	75.0	77.4	71.3
Wo	42.15	42.39	42.30	39.45	40.82	42.67	42.10	47.67	45.31	42.92	40.15	44.13	41.56
En	42.24	45.09	39.26	47.65	43.90	47.98	45.03	44.97	46.86	43.19	44.85	43.25	41.68
Fs	15.61	12.52	18.44	12.90	15.28	9.35	12.87	7.36	7.83	13.89	15.00	12.62	16.76

Note: 1–3 Stena Volcano (sample S-564); 4–5 dike in the Karymskii caldera wall (sample k10-05); 6–7 Ditmara Volcano (sample 21-99l); 8–10 4800 tephra (sample k6-06); 11–13 1996 tephra (sample k17-96). Magnesia coefficient: $Mg^{\#} = Mg/(Mg + Fe)$, at. %. Pyroxene minals: Wo wollastonite, En enstatite, Fs ferrosilite. For the other legend see Table 1.

Orthopyroxene is extremely rare among the KVC phenocrysts and olivine basalts (Fig. 4a). It was found in the 1996 basalts and in the poorly crystallized basaltic andesites of the Early Holocene tephra [9]. The precaldera basalts and the 4800 tephra contain Opx only in the form of solid-phase inclusions ($Mg^{\#}$ 77–82) in clinopyroxene ($Mg^{\#}$ 78–83). An unusually high-alumina (Al_2O_3 6.7%, $Mg^{\#}$ 85 and no Na_2O) orthopyroxene (alumobronzite) is found as a crystalline inclusion in the $Mg^{\#}$ 78 clinopyroxene in the Stena basalts.

Spinellide occurs in basalts mostly as solid-phase inclusions in olivine, clinopyroxene, and plagioclase, more rarely as daughter phases in partially crystallized melt inclusions. The spinellide vary in size within 5–30 μm, occasionally there are larger segregations. The grains are oval and octahedral. Olivine growths in basalts of the 4800 tephra contain some isolated spinel grains as large as 70–100 μm in the intergrain space. Below we mostly discuss the compositions of spinellide in olivine, and to a lesser degree in anorthite. These vary in a wide range and show a compositional series typical of each object of study, from chromite and chromopicotite through subalumochromite to hercynite on the one hand and from subferrichromopicotite through subferrialumochromite to chromomagnetite and chrome-bearing titanomagnetite on the other (Fig. 5a,

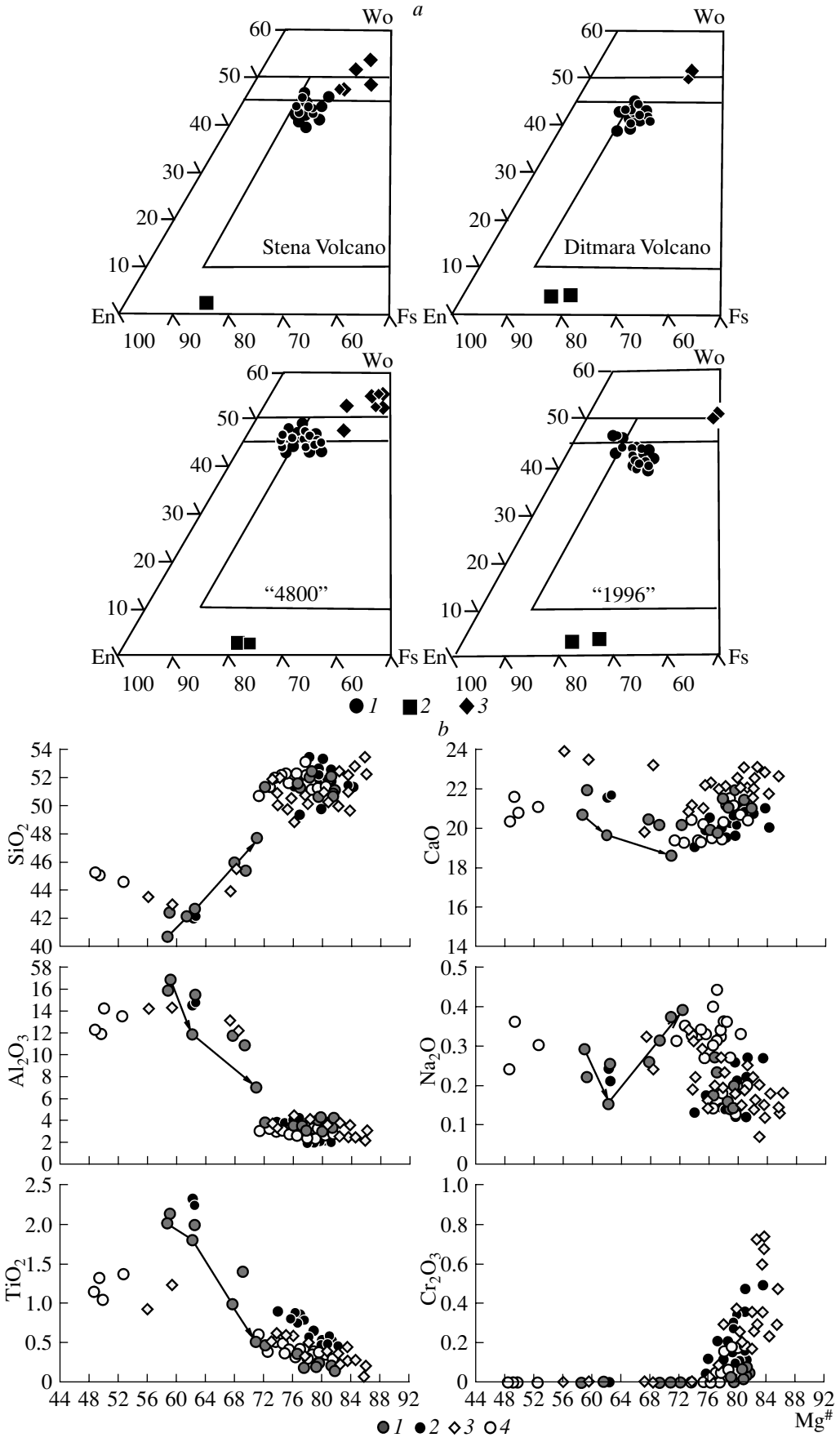
a
Wo
En
Fs
Stena Volcano
Ditmara Volcano
"4800"
"1996"
1
2
3
b
SiO2
CaO
Al2O3
Na2O
TiO2
Cr2O3
Mg#
1
2
3
4

Table 4). We have detected a difference in spinel composition in olivine from the basalts of the northern and southern sectors of the KVC. Occasional solid-phase spinel inclusions in olivine of the Fo 78–82 basalts from Stena and Malyi Semyachik consist of alumina varieties ($Al^{\#}$ 0.61–0.72, $Mg^{\#}$ 0.47–0.54, $Cr^{\#}$ 0.15–0.20). The concentration of Al_2O_3 in these are 32.5–41.5% and that of TiO_2 is 0.37–0.59%. Solid-phase hercynite inclusions with still higher alumina content (Al_2O_3 44–47%, TiO_2 0.39–0.71%) were found in anorthite phenocrysts in the k10-05 basalt sampled from the northwest wall of the Karymskii caldera. They occupy the lowest position along the $Al–Fe^{+3}$ side in the diagram (Fig. 5a), tending toward the region of maximum aluminum. The solid-phase spinellid inclusions in the olivine subphenocrysts that were crystallized later show increasing concentrations of theoretical ferrous oxide, along with low chrome content and decreased alumina content.

The magnesia olivines (Fo 85–89) found in basalts in the southern sector of the Karymskii Volcanic Center (Ditmara Volcano, the 4800 tephra) contain chromous spinellide. The highest chrome concentrations were found in chromites and chromopicotites in olivines from the 4800 basalts ($Cr^{\#}$ 0.51–0.7, $Mg^{\#}$ 0.48–0.69). The content of chrome oxide in these reaches 43–51%, the figure for TiO_2 being 0.27–0.64%. They form a compact swarm of composition points in the diagram (Fig. 5a), suggesting their crystallization during a definite phase and in comparatively stable environments. While the concentrations of $Mg^{\#}$ and chrome oxide decrease in olivines containing more iron, the chrome content in spinel remains nearly unchanged. An exception is low-magnesia, low-chrome titanium-bearing spinellide from ferriferous olivine phenocrysts (Fig. 5b). The spinels of the 4800 basaltic tephra (having the highest chrome content) tend toward the spinel field from olivines of the basaltoids found on Klyuchevskoi Volcano [21]. Spinel grains from intergrain zones of olivine growths (4800 tephra) are zonal. The grain nucleii have a chromous composition, while the marginal zones of the crystals show increased concentrations of iron. The spinels in olivines from the Ditmara basalts consist of subalumochromites. As the content of magnesia in olivines decreases, the spinel compositions are moving toward lower concentrations of Cr_2O_3 (from 36.0 to 26.7 wt %), Al_2O_3 (from 21.3 to 13.5 wt %), and MgO (from 12.7 to 7.8 wt %) accompanied by an increasing iron content (from 33.3 to 54 wt %) and increasing concentrations of TiO_2 (from 0.64 to 2.04 wt %), while the $Cr^{\#}$ decreases only slightly, from 0.51 to 0.40 wt %. The olivines from the 1996 basalts are represented by varieties of still higher alumina content (subferrialumochromites). Their evolutionary trend, which is related to enrichment with iron oxides and titanium oxides, is continuous, demonstrating that the melt was being gradually enriched with these components.

Titanomagnetite is present in the groundmass of the basalts. This is chrome-bearing in basalts of the southern sector and chrome-less in those of the northern, but with an increased titanium concentration. The increasing titanium concentration during crystallization is also reflected in the appearance of ilmenite in the groundmass.

MELT INCLUSIONS IN OLIVINES

The present study is mostly concerned with inhomogeneous melt inclusions in olivine. The inclusions have rounded shapes, their sizes vary between a few μm and 10–20 μm, more rarely 30–40 μm. These latter sizes are generally rather rare, but are abundant in olivines of the 1996 basaltic tephra. The melt inclusions are generally crystallized to varying degrees and consist of crystalline phases, residual glass, and the open cavities of gas bubbles (Fig. 6, Table 5). The daughter crystalline phases consist of fassaite (high alumina, with high concentrations of calcium and titanium Cpx, occasionally associated with spinellide). Fassaite, when found in inclusions, forms isolated needle-shaped microlites, clusters of needle-shaped microlites of skeletal appearance, and isolated larger phases. The inclusions that have been crystallized to the greatest extent are typical of olivine Fo 78–82 from the Stena basalts (Fig. 6c, 6d) and Fo 85–87 from the 4800 basaltic tephra. In these inclusions, fassaite occasionally fills half the volume of an inclusion. An inclusion was found in the Stena olivines where fassaite crystallized from the boundary with the host olivine, forming a growth in the margin with another idiomorphic zonal fassaite crystal, which is in turn in a common growth with aluminiferous pleonaste spinel (Fig. 6d). A zonal fassaite crystal (Table 5, nos. 6, 7) shows magnesia content increasing away from the center (58.7) toward the edges (70.9), while the concentrations of aluminia, iron, and titanium are decreasing, approaching the concentrations of these components in clinopyroxene phenocrysts. In the marginal zone the concentration of Na_2O increases to reach the content of that component in clinopyroxenes of the 1996 basalts. The content of Al_2O_3 in the pleonaste

Fig. 4. Composition of clinopyroxene phenocrysts. Mg–calcium–iron relationship (En–Wo–Fs) in pyroxenes of olivine basalts in the Karymskii Volcanic Center(*a*): (*1*) clinopyroxene phenocrysts, (*2*) orthopyroxene, solid-phase inclusions in clinopyroxenes, (*3*) high-alumina clinopyroxene (fassaite), daughter phase in partially crystallized inclusions in olivine. The oxide relationship in clinopyroxene versus its magnesia content ($Mg^{\#}$) (*b*): (*1*) Stena and Malyi Semyachik volcanoes, (*2*) Ditmara Volcano, (*3*) 4800 basalts, (*4*) 1996 basalts. Figurative points with $Mg^{\#} > 70$ are phenocrysts, those with $Mg^{\#} < 70$ are fassaites, daughter crystalline phases in melt inclusions in olivine. Arrows show compositional variation in the zonal fassaite crystal from a partially crystallized inclusion in olivine of Stena basalt.

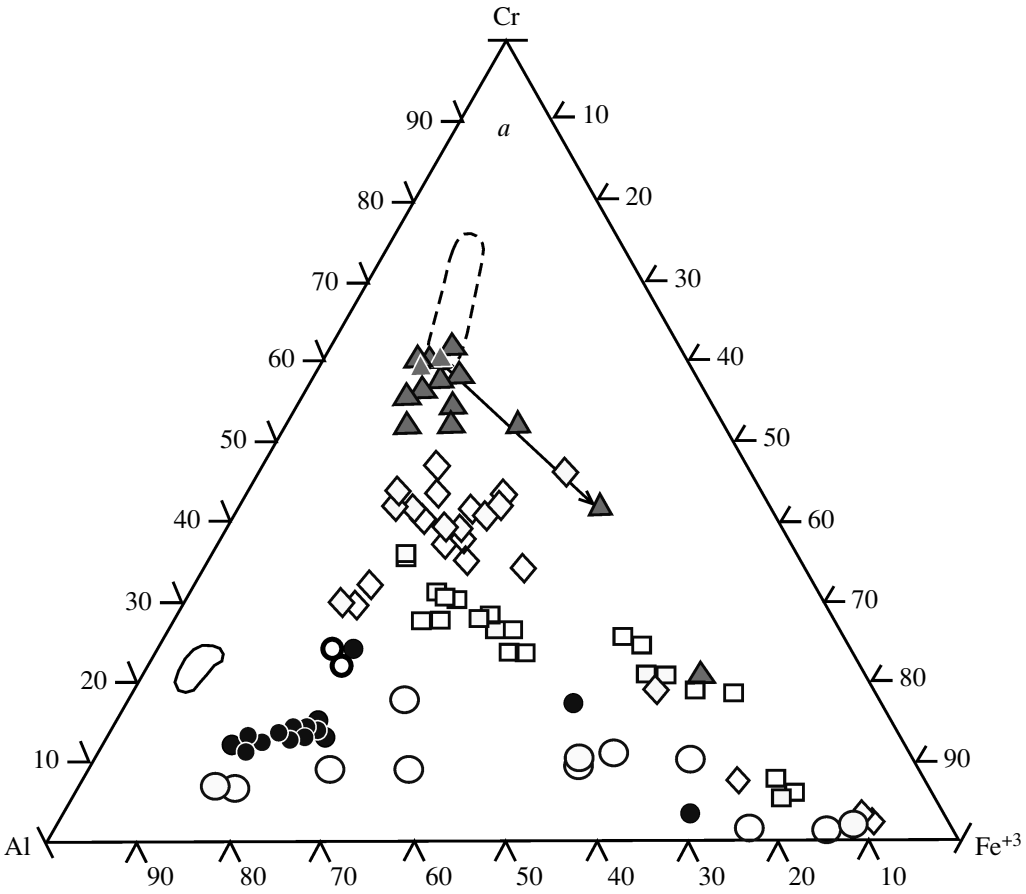
Cr
a
Al
Fe+3
90
80
70
60
50
40
30
20
10

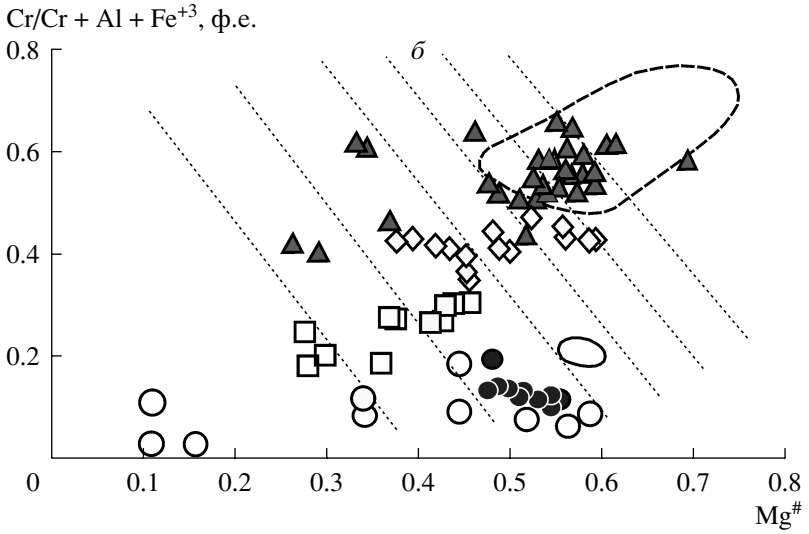
Cr/Cr + Al + Fe+3, ф.е.
б
Mg#
0.8
0.6
0.4
0.2
0
0.1
0.2
0.3
0.4
0.5
0.6
0.7
0.8

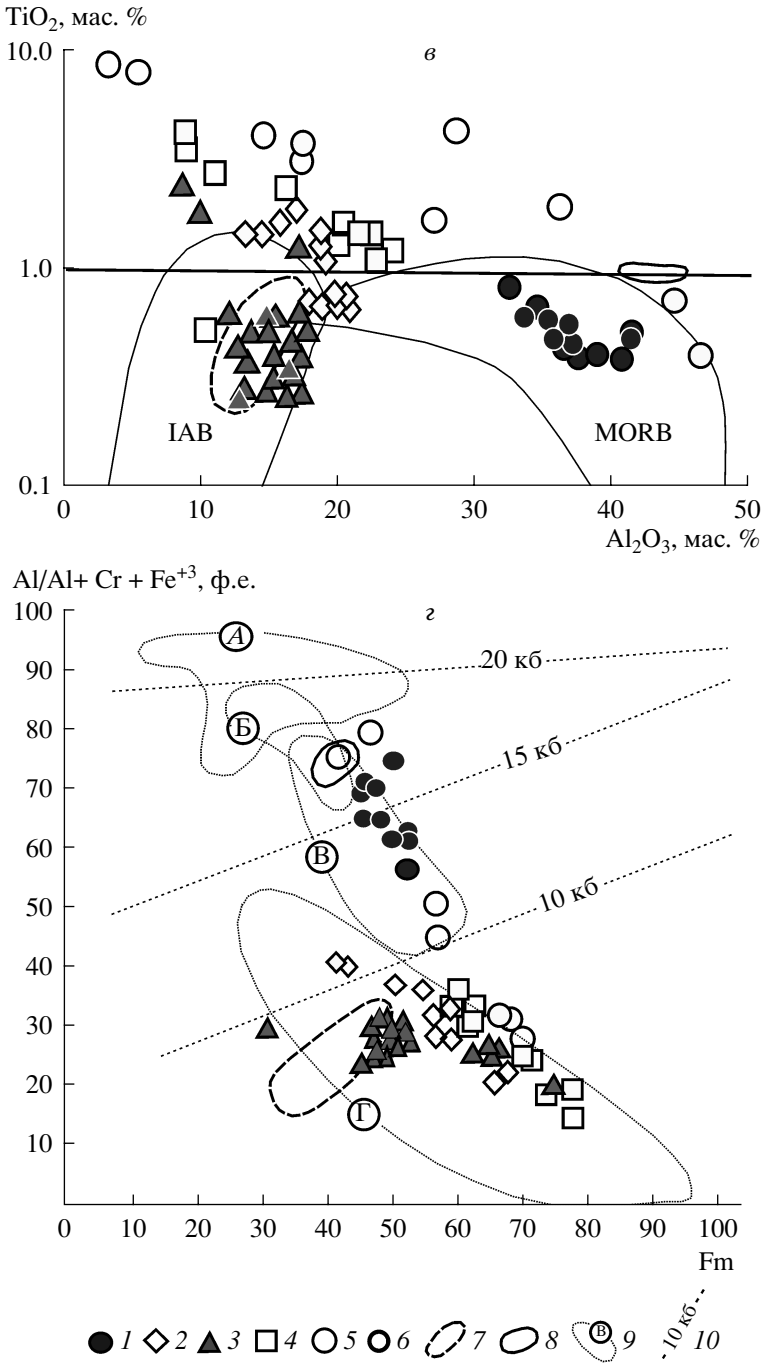

Fig. 5. Spinellid composition (solid-phase inclusions in olivines of the Karymskii Volcanic Center basalts studied here). The Al-Cr–Fe^{+3} diagram in spinels (*a*): (*1*) Stena and Malyi Semyachik volcanoes, (*2*) Ditmara volcano, (*3*) 4800 basalts, (*4*) 1996 basalts, (*5*) dike on Proto-Karymskii Volcano, sample k10-05, (*6*) aluminiferous spinel in olivines of alkali basalts in the lower section of the Shchapina suite [5]. Fields: (*7*) spinels from Klyuchevskoi lavas [21], (*8*) spinels in Cretaceous alkali basalts of the Kamchatskii Mys Peninsula, sample D213-17 [17]. The arrow shows the compositional variation in a spinel grain in an olivine growth, the 4800 basalt; the legends 1 through 8 also apply later. The relationship of chrome content ($Cr^{\#}$) and magnesia content ($Mg^{\#}$) in spinels (*b*). Thin dashed lines are isopleths of Fo content in host olivine associating with spinels. The TiO_2-Al_2O_3 diagram in spinels (*c*). IAB and MORB are spinel fields for island arc basalts and mid-oceanic ridge basalts, respectively, after [27]. The alumina ($Al^{\#}$)–iron (Fm) diagram for spinel (*d*): (*9*) spinel fields for different types of xenoliths and plutonic hyperbasites in Kamchatka and other regions after [12]: (@A) lherzolites in Vietnam basanites, (@B) harzburgites and pyroxenites for Kharchinskii Volcano, (@C) verite–pyroxenite association in the area of Bakening Volcano, (@D) harzburgites and pyroxenites for Klyuchevskoi Volcano; (*10*) hypothetical boundaries of barophile fields, the estimate was made with the help of a spinel–pyroxene geobarometer [28]. $Cr^{\#}$= Cr/Cr + Al + Fe^{+3}, $Mg^{\#}$= Mg/Mg + Fe^{+2}, $Al^{\#}$= Al/Al + Cr + Fe^{+3}, Fm = Fe/Fe + MgKey: (1) in dec. units; (2) b; (3) wt %; (4) c; (5) kbars; (6) d

Table 4. Representative compositions of spinel inclusions (wt %) in phenocrysts from basalts of the Karymskii Volcanic Center

Components	1	2	3	4	5	6	7	8 c	9 mar	10	11	12	13	14
TiO_2	1.45	0.47	0.83	0.51	1.63	1.05	0.64	0.37	2.34	0.45	0.55	0.31	1.55	1.66
Al_2O_3	26.28	36.42	39.28	46.72	26.82	18.73	19.98	13.37	8.92	14.00	17.91	15.44	10.57	20.36
Fe_2O_3	25.15	18.61	15.49	13.34	24.47	22.43	13.53	10.04	28.76	18.00	12.32	8.85	42.37	22.81
FeO	22.42	20.38	20.10	18.67	21.92	20.61	17.09	24.44	27.50	20.68	17.87	14.78	25.00	21.96
Cr_2O_3	15.52	12.22	12.57	6.67	13.97	26.66	35.95	46.40	27.79	37.72	39.62	48.09	14.93	22.90
MgO	9.60	11.28	12.16	13.56	9.61	9.47	11.74	6.83	5.84	8.65	10.98	12.91	5.23	9.09
MnO	0.25	0.17	0.23	0.00	0.24	0.20	0.29	0.40	0.25	0.45	0.44	0.50	0.22	0.03
NiO	0.00	0.00	0.00	0.00	0.00	0.00	0.00	0.00	0.00	0.00	0.00	0.00	0.00	0.00
ZnO	0.00	0.00	0.09	0.00	0.00	0.00	0.00	0.00	0.00	0.00	0.01	0.00	0.00	0.00
Total	100.67	99.55	100.75	99.47	98.66	99.15	99.22	101.85	101.40	99.95	99.70	100.88	99.87	98.81
Fo (An)	78.5	79.5	79.5	(90.0)	80.7	80.0	84.2			79.1	85.5	88.7	74.3	80.9

Note: 1–3, 5–14 spinel inclusions in olivine phenocrysts, 4 spinel inclusion in an anorthite phenocryst; 1–3 Stena Volcano (sample S-564); 4–5 dike in the Karymskii caldera wall (sample k10-05); 6–7 Ditmara Volcano (sample 21-99l); 8–12 4800 tephra (sample k6-06); 8–9 spinel subphenocryst; 13–14 1996 tephra (sample k17-96); Fo and An denote forsterite and anorthite minals of olivine and plagioclase phenocrysts with spinel inclusions. For the other legend see Table 1.

reaches 54.13 wt %. The 1996 basalts have abundant subalumochromomagnetites (Al_2O_3 6-9 wt % and Cr_2O_3 5–12 wt %) in melt inclusions concurrently with fassaite microlites. Occasionally spinellid grains intersect the boundaries of the melt inclusions, indicating that they are present there as a captured phase. A partially crystallized melt inclusion with a fassaite daughter phase was also found in a solid-phase spinel inclusion in an anorthite phenocryst from the k10-05 basalt (the dike in the northwest wall of the Karymskii caldera, Fig. 6f).

All inclusions have fassaite with increased concentrations of Al_2O (12–16.5 wt %), TiO_2 (1–2.4 wt %), FeO (8.6–14.4 wt %) (Table 5). Its $Mg^{\#}$ correlates with that of the host olivine, varying between 48.6–52.6 in the 1996 tephra and 56–69.7 in high-magnesia basalts (Fig. 4b). It can be seen in the plots that fassaite typically exhibits an inflection in the $Mg^{\#}$ 62 region. We suggest an incipient crystallization in melt inclusions of both plagioclase and Fe–Ti oxides as the cause of a dramatic drop in the concentration of Al_2O_3, CaO, and TiO_2 during further decrease in the concentration of magnesia in the fassaite. Plagioclase (bitownite) was detected in the 1996 basalts among daughter phases in melt inclusions contained in olivines Fo 74–76 (Fig. 6e, Table 5).

The composition of residual glass in the melt inclusions depends on the degree of crystallization in them (Table 5). With the lowest concentration of daughter crystalline phases, the content of SiO_2 in residual glass varies within the range 50.7–52.4% and has an aluminiferous composition (20–22 wt % Al_2O_3, 12–14 wt % CaO). As the degree of crystallinity increases, the residual glass is oxidized to reach the basaltic andesite composition (54.6–56.9 wt % SiO_2). As MgO decreases in the glass, a moderate increase in SiO_2, Al_2O_3, CaO, and TiO_2 occurs and a decrease in FeO and Na_2O. The inclusions with a high degree of crystallization have much higher concentrations of SiO_2 (dacite and rhyodacite compositions) and Na_2O, while those of Al_2O_3, CaO, TiO_2, and FeO decrease. The residual glass occasionally has increased concentrations of K_2O and water (glass "burns" during micrologging analysis).

BASALT PETROCHEMISTRY AND GEOCHEMISTRY

The olivine basalts of the Karymskii Volcanic Center are low- and moderate-potassium basalts of normal alkalinity in the sodium series (Na_2O/K_2O = 4–7), and belong to the tholeiite series in their FeO^*/MgO ratio (1.0–2.9). Some isolated basaltic compositions, mostly in the KVC southern sector, have increased concentrations of SiO_2 and K_2O, and occur at the boundary between the tholeiite and the calc-alkali series. The Stena and Malyi Semyachik basalts typically are the lowest in silica and high in magnesia (MgO ranging from 11.1 wt % in high-magnesia basalts to 3.5 wt % in leucocratic ones; Al_2O_3 is 16 to 22.7 wt %, respectively) (Fig. 7a, Table 6). The basalts in the southern sector, except for the highest-magnesia Ditmara varieties, continue the evolutionary trend of the Stena and Malyi Semyachik basalts, and belong to aluminiferous varieties. Also in this set is the dike in the northwest wall of the Karymskii caldera. In their concentrations of macrocomponents, the basic lavas in the KVC southern sector are similar to the pre-caldera olivine basalts in the Uzon–Geyser volcano-tectonic depression [8], being different in having higher concentrations of CaO, MgO, and Na_2O. As the concentration of silicic acid increases

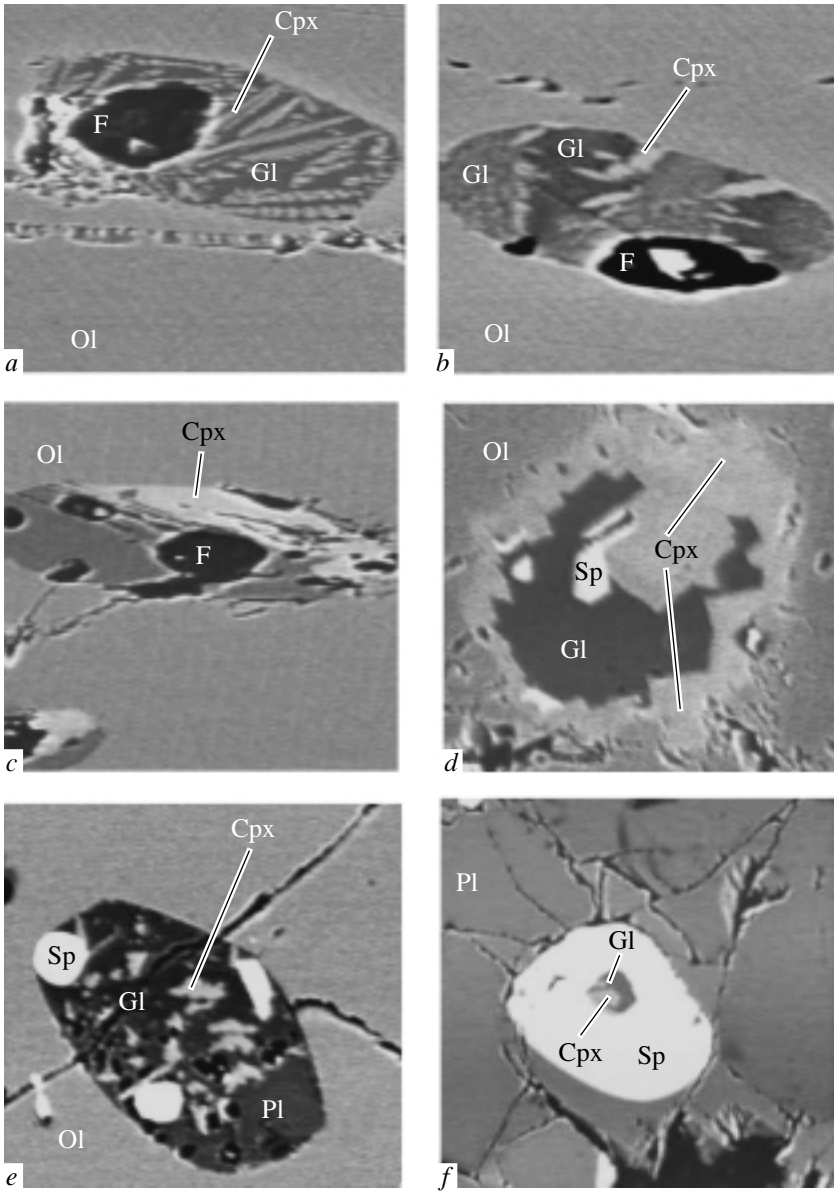

Fig. 6. Microphotographs of melt inclusions: in olivine (*a–d*, Stena Volcano; @e 1996 tephra); in anorthite (*f* dike k10-05). Indices of crystalline phases: Ol host olivine, Cpx crystalline daughter phase of clinopyroxene (fassaite), Gl residual glass, F opened cavities of gas bubbles, Sp spinel, crystalline daughter phase, Pl in (*e*), host mineral, anorthite. Image size: *a* to *d* 50 μm, *e* 100 μm, *f* 200 μm.

in basalts, so do those of many rare lithophile elements, most notably Sr, Zr, Nb, and Y; the concentrations of iron elements decrease (V, Ni, Co, and Sc) (Fig. 7b, Table 6). Concurrently, the basalts of the northern sector show a parallel trend in the distribution of some rare elements, expressed in a more rapid decrease in the concentrations of Ni and Co as the lavas become lower in alumina and contain greater amounts of V and Y. The distribution of Cr in the KVC basalts shows that the moderate-magnesia basalts of Ditmara Volcano (the southern sector) are much more enriched in that component than are the melanocratic varieties of Stena and Malyi Semyachik volcanoes (the northern sector). This pattern is consistent with the compositions of solid-phase spinel inclusions in olivines from basalts found in different KVC sectors.

The distribution spectra for rare-earth elements (REE) normalized by chondrite highlight three types of curves for the KVC basalts (Fig. 8a). The first type includes the spectra of the Stena melanocratic basalts. They typically have the lowest content of REE (21.4–22.4), a poor fractionation of these (La/Yb 1.7–2.6), a slight deficit in light lanthanids (La/Gd 1.14–1.3) and a greater depletion (Gd/Yb 1.5–1.6) in heavy lanthanids. This spectrum is characteristic for primitive melts whose crystallization differentiation mostly involves olivine and clinopyroxene [3]. The second type

Table 5. Compositions of residual glass and crystalline phases (wt %) in unhomogenized melt inclusions in olivine

Components	1	2	3	4	5	6	7	8	9	10	11	12
SiO_2	52.74	64.22	67.49	58.43	54.63	41.74	47.78	44.82	45.16	46.61	0.00	0.00
TiO_2	1.30	0.15	0.13	1.30	1.39	2.05	0.51	0.95	1.32	0.00	0.18	5.25
Al_2O_3	22.04	18.75	18.27	20.34	22.99	16.50	7.04	12.23	11.21	33.89	54.11	8.72
FeO^*	4.68	1.52	1.23	4.42	2.57	11.35	9.88	9.19	14.40	1.26	34.44	68.60
Cr_2O_3	0.00	0.00	0.00	0.00	0.00	0.00	0.00	0.00	0.00	0.00	0.00	12.21
MgO	2.07	0.28	0.24	1.39	0.85	9.06	13.53	12.24	7.87	0.00	10.58	5.73
CaO	12.74	3.78	3.25	10.14	14.96	21.08	18.60	20.07	21.68	18.20	0.06	0.00
Na_2O	3.46	5.23	3.65	2.69	2.64	0.24	0.37	0.25	0.36	1.51	0.00	0.00
K_2O	0.57	3.35	3.49	0.85	0.64	0.00	0.04	0.00	0.00	0.04	0.00	0.00
Total	99.60	97.28	97.75	99.56	100.72	102.02	97.75	99.75	102.00	101.51	99.37	100.51
Fo	77.6	81.4	81.4	78.8	78.4	81.4	81.4	87.5	74.3	74.3	81.4	74.3

Note: 1–5 residual glass in melt inclusions in olivine: 1–3 Stena Volcano (1 inclusion with needle-shaped fassaite microlite, 2 inclusion with a zonal fassaite crystal, center of the inclusion, 3 same, near the fassaite crystal); 4–5 Ditmara Volcano, partially crystallized inclusions, 6–9 crystalline phases of fassaite and high-alumina augite; 6–7 Stena Volcano (6 zonal crystal, center, 7 same, margin); 8 4800, 9 1996, partially crystallized inclusion. 10 1996, plagioclase phase in the inclusion. 11–21 spinellid phases in melt inclusions: 11 Stena Volcano, pleonaste (together with zonal fassaite, 6–7), 12 1996, subferrialumochromite. Fo forsterite minal of host olivine.

includes the spectra of moderate-magnesia basalts discharged by Stena, Malyi Semyachik, and Ditmara volcanoes and the spectra of aluminiferous basalts in the dike situated in the northwest wall of the Karymskii caldera. These spectra typically have steep curves from light lanthanids to intermediate ones (La/Gd 2.1–2.8) and some flattening toward the heavier REE (Gd/Yb 1.7–1.8). The REE concentrations are increasing with increasing concentration of silicic acid in the basalts from 26.7 to 46.8 g/t. The Ditmara basalts have REE concentrations similar to those in the Malyi Semyachik basalts (41.6), with the concentration being the highest in the dike. This increase in the REE concentrations is mostly due to a dramatically increased content of light lanthanids, which is related to an increasing role of plagioclase in melt fractionation [3] and is consistent with the higher alumina content for this set of basalts. The third type of spectra is distinguished by the highest REE concentration (46.3–46.8) and is related to aluminiferous basalts of explosive eruptions (4800 and 1996). One characteristic feature of these spectra is a dramatic decrease in the concentrations of elements in the middle part of the series (La/Gd 2.9–3.0) and subsequent flattening in the region of heavy earths (Gd/Yb 1.6–1.7). The depletion in heavy REE may be caused by concurrent fractionation of plagioclase and the dark minerals, mostly pyroxene. All the spectra have no europium anomaly.

The low REE concentrations in the magnesia basalts of the northern sector (Stena and Malyi Semyachik) and the deficit of light lanthanids in them are features similar to those for the tholeiites of mid-oceanic ridges (MORB). Judging by the Th/Yb vs. Ta/Yb relationship [29], the basalt compositions of the Karymskii Volcanic Center and of volcanoes in the northern part of the Eastern volcanic belt and the Central Kamchatka depression [22] are similar to the composition of a depleted mantle source (Fig. 8c). The positions of their compositions outside the mantle relation field indicates fluid enrichment for basaltic melts caused by dehydration of the plunging oceanic plate. The basalts of the KVC southern sector when plotted in the Th/Yb vs. Ta/Yb diagram are situated in the field of basalt compositions for the Sredinnyi Range of Kamchatka [22], which largely reflects their greater differentiation.

The distribution curves for hygrophile and magmatophile elements (Fig. 8b) have similar configurations showing pronounced Nb and Ta minima and well-expressed maxima in the distribution of Ba, K, Pb, and Sr, which is characteristic for magmas of island-arc geodynamic settings whose generation involved supra- 3
subduction fluids [24]. One notes a Y minimum in the Stena basalts of highest magnesia concentration, which when combined with the low concentration of heavy REE in them may indicate a harzburgite restite of the primary magmas and high degrees of mantle melting [23]. Similar distributions of magmatophile elements in the KVC basalts indicates their generation due to common magma generation processes.

RESULTS AND DISCUSSION

Studies in the composition of rock-forming minerals in application to olivine basalts during different phases in the KVC evolution show that the minerals typically have similar evolutionary trends, indicating a genetic affinity among the primary basaltoid melts and similar crystallization processes. The trend directions are consistent with the existing notions of fractional crystallization with decreasing temperature as one of

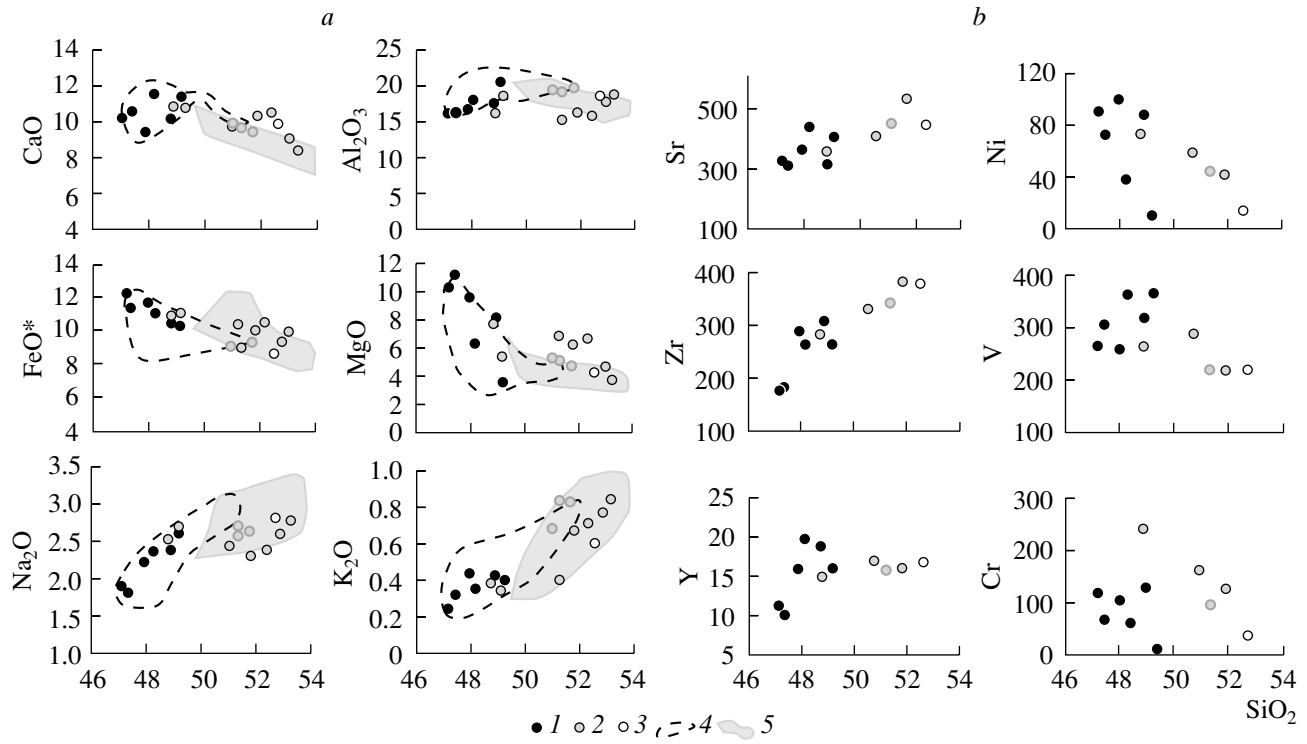

Fig. 7. Concentrations of major components (*a*) and rare elements (*b*) in relation to SiO@2 concentration (wt %) in olivine basalts of the Karymskii Volcanic Center: (*1*) Stena and Malyi Semyachik (northern sector), (*2*) basalts of the southern sector, 1996 tephra is in bolder circles, (*3*) basalt of the dike in the northwest wall of the Karymskii caldera, (*4*) field of olivine basalts after [18], (*5*) olivine basalts of the Uzon–Geyser depression [8].

the basic parameters that controls the directions of evolution for the melts. An analysis of coexisting crystalline phases (growths and solid-phase inclusions in minerals) shows that process is related to cotectic mineral association Pl–Ol–Cpx. All the basalts considered here exhibit an omnipresent association of these minerals with the composition Ol ($Mg^{\#}$ 74–78)–Cpx ($Mg^{\#}$ 76–78)–Pl (An 77–89). The association corresponds to gabbroid intrusive series and can be regarded as deriving from a crustal magma chamber at a pressure of 2–5 kbars [1], corresponding to depths of 7–18 km. The dominance of moderate-magnesia olivine phenocrysts ($Mg^{\#}$ 75–82) in melanocratic basalts (MgO 9–11 wt %) for the Stena and Malyi Semyachik volcanoes may indicate that most of these are disequilibrium phases. According to [26], olivines with $Mg^{\#}$ 85–86 may be in equilibrium with such melts (a single olivine Fo 85 grain with an inclusion of aluminiferous spinel has been found in the Stena basalts [18]). As well, there is also a disequilibrium mineral association estimated from the composition of coexistent solid-phase inclusions: Ol ($Mg^{\#}$ 80–82, more rarely 85)–Cpx ($Mg^{\#}$ 80–82)–Pl (An 89–96). It is also a derivative of magmas supplied by shallow crustal magma chambers.

The more differentiated silicic basalts in the southern sector typically have a wide range of magnesia content in olivines and clinopyroxenes, especially for Ditmara lavas and the 4800 tephra. Along with low-magnesia phenocrysts one finds abundant phenocrysts of olivine with $Mg^{\#}$ 85–89 and clinopyroxene with $Mg^{\#}$ 84–86. Plagioclase has not been detected in association with these, either as growths or solid-phase inclusions. This too is a disequilibrium association in its lava composition, and obviously crystallized from melts of higher magnesia content. According to [26], it is the olivine $Mg^{\#}$ 78–80 which is in equilibrium in the moderate-magnesia Ditmara basalts having 7–8% of Mg in the melt.

Rare (but characteristic for all olivine basalts in the Karymskii Volcanic Center) solid-phase inclusions of orthopyroxene ($Mg^{\#}$ 77–82) in augites of similar magnesia content show that that mineral was present during an earlier crystallization phase of the basaltic melt, as has also been noted for basalts of Klyuchevskoi Volcano [21].

The composition of solid-phase spinellid inclusions in olivines is the most informative in the basalts studied. The basalts of the southern sector have olivines that mostly contain chromous spinellide, which include chromites, chromopicotites, and subalumochromopicotites. A high-chrome spinel was found in the highest-magnesia olivines (Fo 86–89) from the 4800 basaltic tephra. It is similar to the Klyuchevskoi chromous spinels (Fig. 5) in its level of chrome content ($Cr^{\#}$ 0.57–

Table 6. Concentrations of major (wt %) and rare elements (g/t) in basalts of the Karymskii Volcanic Center

No.	S-567	S-564	S-571@б	S-570a	S-608	S-576	21–99l	22–99l	@к27–96	@к13–97	@к10–05
SiO_2	47.17	47.37	48.89	49.14	47.91	48.19	48.85	50.73	51.36	51.84	52.61
TiO_2	0.75	0.64	0.82	0.87	0.78	0.95	0.81	0.91	0.89	0.55	0.76
Al_2O_3	16.17	16.22	17.38	20.62	16.81	18.02	16.71	17.20	19.43	16.25	18.90
Fe_2O_3	4.30	3.02	3.39	5.48	3.78	3.69	3.67	3.70	1.99	3.02	3.92
FeO	7.72	8.26	7.00	4.67	7.72	7.18	6.51	5.77	6.99	6.99	4.76
MnO	0.20	0.19	0.18	0.16	0.19	0.19	0.16	0.17	0.12	0.15	0.15
MgO	10.30	11.10	7.94	3.47	9.63	6.42	7.71	6.70	5.10	6.38	4.30
CaO	10.54	10.71	10.67	11.62	9.58	11.85	11.1	10.30	9.94	10.52	10.20
Na_2O	1.92	1.81	2.39	2.61	2.23	2.38	2.52	2.66	2.58	2.30	2.81
K_2O	0.26	0.31	0.41	0.39	0.42	0.34	0.40	0.52	0.84	0.68	0.62
P_2O_5	0.08	0.07	0.11	0.10	0.13	0.13	0.11	0.23	0.13	0.10	0.15
LOI	0.43	0.45	0.79	0.73	0.55	0.49	1.64	1.09	0.19	1.12	0.88
Total	99.85	100.14	99.97	99.86	99.71	99.83	100.19	99.98	99.56	99.9	100.06
Sc	34	31	39	31	27	43	36	35	26	31	26
V	266	305	319	346	258	362	262	279	222	218	224
Cr	113	67	126	7	102	59	244	160	97	124	41
Co	57	56	45	27	53	42	38	38	25	27	26
Ni	89	72	88	8	99	36	74	59	43	41	15
Cu	97	132	146	131	75	157	124	149	105	104	79
Zn	86	80	92	79	83	91	66	70	142	74	65
Ga	15.6	15.5	19.5	20.4	17.9	20.0	15.9	19.1	17.4	21.5	17.5
Ge	1.1	1.1	1.2	0.9	1.1	1.3	1.1	1.3	1.0	1.3	1.5
Rb	3	2	5	2	5	4	5	7	8	10	9
Sr	307	285	396	385	349	421	339	402	442	519	436
Y	11	10	19	16	16	20	15	17	16	16	17
Zr	26	25	51	42	47	43	47	56	58	66	66
Nb	0.7	0.8	1.3	1.0	1.6	1.4	1.6	1.9	1.8	1.8	2.0
Mo	1.0	0.7	1.0	0.5	0.8	0.5	0.9	1.0	1.7	1.2	0.8
Sn	0.8	0.5	0.7	0.6	0.7	0.6	0.4	1.0	1.4	0.9	0.9
Sb	0.4	0.4	0.6	0.5	0.5	0.5	1.8	1.3	1.7	1.9	0.5
Cs	0.18	0.11	0.28	0.21	0.29	0.27	0.35	0.30	0.33	0.37	0.27
Ba	102	94	132	115	129	121	118	126	177	186	166
La	2.29	1.94	4.24	3.07	4.20	3.92	5.66	5.27	6.63	6.75	5.81
Ce	5.88	5.38	11.12	8.31	10.80	11.16	13.56	12.72	16.37	15.62	14.65
Pr	0.91	0.87	1.74	1.34	1.64	1.75	1.81	1.84	2.22	2.17	2.10
Nd	4.61	4.25	8.55	6.82	8.13	8.55	8.21	8.48	9.76	9.68	9.50
Sm	1.35	1.40	2.45	2.08	2.14	2.69	2.20	2.30	2.31	2.31	2.73
Eu	0.48	0.50	0.88	0.78	0.79	0.96	0.75	0.79	0.77	0.75	0.91
Gd	1.69	1.70	2.96	2.67	2.64	3.18	2.51	2.55	2.26	2.33	2.76
Tb	0.30	0.31	0.50	0.44	0.43	0.54	0.43	0.41	0.38	0.40	0.47
Dy	1.89	2.00	3.16	2.78	2.63	3.45	2.54	2.61	2.35	2.54	3.00
Ho	0.41	0.42	0.66	0.59	0.55	0.72	0.53	0.54	0.50	0.52	0.61
Er	1.16	1.17	1.93	1.69	1.60	2.05	1.51	1.48	1.37	1.45	1.70
Tm	0.17	0.18	0.28	0.25	0.23	0.30	0.22	0.22	0.23	0.21	0.25
Yb	1.11	1.13	1.74	1.60	1.47	1.92	1.44	1.40	1.44	1.34	1.62
Lu	0.17	0.16	0.27	0.23	0.23	0.29	0.22	0.22	0.21	0.21	0.24
Hf	0.67	0.70	1.31	1.07	1.22	1.15	1.37	1.55	1.59	1.75	1.88
Ta	0.05	0.07	0.11	0.08	0.11	0.09	0.14	0.18	0.16	0.19	0.16
W	0.09	0.07	0.11	0.06	0.27	0.07	0.70	0.76	0.77	0.92	0.09
Tl	0.02	0.02	0.04	0.03	0.04	0.04	0.04	0.03	0.06	0.05	0.03
Pb	3.46	2.30	2.59	1.78	2.16	2.33	1.57	2.36	1.96	2.87	2.73
Th	0.39	0.25	0.43	0.29	0.44	0.33	0.84	0.63	0.82	0.90	0.68
U	0.19	0.15	0.23	0.16	0.25	0.18	0.26	0.29	0.44	0.47	0.36

Note: S-567 to S-576: basalts of the KVC northern sector, O.B. Selyangin's samples, 21-99l to k13-97: basalts of the KVC southern sector, k10-05: basalt of the KVC central sector. For the analytical methods used see main text.

0.68), the extent of oxidation (FeO/Fe_2O_3 1.8–2.5), and a low concentration of TiO_2 (0.27–0.4 wt %); we remember that Klyuchevskoi primary picrite melts were found to crystallize at the upper mantle level [21]. The compact isolation of spinel compositional points in the diagram (Fig. 5a) indicates stable environments of melt crystallization. The temperature of crystallization was calculated from the geofugometer Ol–Sp [25] within 1300°C at –6.35 / + 1.17 QFM as the oxygen fugacity. No paragenesis of Ol-Sp, whose composition would be relevant to the mantle levels [23] has been detected, but the high value of $Cr^{\#}$ for the liquidus spinel indicates that the source of primary, nearly picritoid, magmas was at the boundary of the crust and upper mantle. Chromous and simultaneously more aluminiferous and ferrous spinellide in the Ditmara basalts and in the 1996 basaltic tephra probably crystallized from melts that were more differentiated and enriched with iron and titanium.

Special interest attaches to the discovery of high-alumina (33–47% Al_2O_3) spinel (hercynite) inclusions in olivine ($Mg^{\#}$ 78–81) from the basalts of Stena and Malyi Semyachik volcanoes and in the anorthite of the k10-05 basalt (the dike in the northwest wall of the Karymskii caldera). High-alumina spinel is not typical of suprasubduction island arc magmas and has not until recently been found in the lavas of other Quaternary volcanoes in the Eastern volcanic belt, both among subphenocrysts and solid-phase inclusions in minerals. In its concentration of alumina ($Al^{\#}$ 0.6–0.78) the spinel found in the olivines and anorthites of the KVC northern sector basalts is similar to that in Late Miocene/Pliocene intraplate alkali basalts (the Shchapina suite) in the eastern spurs of the Valaginskii Range and in the Levaya Zhupanova R. basin [5] and to those found in the Cretaceous basalts (sample D-213-17) in Cape Kamchatskii [17], as well as to the spinel found in ultramafic xenoliths in island arc basalts [12] (Figs. 5a–5d). At the same time, these spinels are different from the aluminiferous spinels in alkali lavas in having a lower concentration of titanium and chrome, and from the spinel found in ultrabasic xenoliths in having a lower magnesia content and higher iron concentrations. The Al_2O_3 vs. TiO_2 classification diagram for low-titanium mantle spinels (Fig. 5c) from [27] shows that the compositions of high-alumina spinels in the basalts of the KVC northern sector are in the field of mid-oceanic ridge basalts (MORB), while the high-chrome spinels found in the 4800 tephra and in Klyuchevskoi lavas are in the spinel field of island arc basalts (IAB).

According to [12], the alumina content ($Al^{\#}$) of spinel is controlled by pressure. Looking at the diagram correlating $Al^{\#}$ and the iron content in the spinels from the ultramafic xenoliths discovered in volcanic rocks of different geodynamic settings (Fig. 5d), one finds that the aluminiferous spinels in the Stena and Malyi Semyachik basalts occur in the spinel field for the verite–pyroxene xenoliths found in volcanites of the intraplate geochemical type. Such spinels crystallize in the pressure range of 12–17 kbars, corresponding to depths of 35–50 km. Those of the highest alumina content, including the solid-phase spinel inclusions in anorthite (the k10-05 basalt), occur in the spinel field of the Cape Kamchatskii alkali basalts [17].

As has been noted, the basalts of the KVC northern sector, whose olivine contains high-alumina spinels, has a composition of mineral associations that classify it as the gabbroid type; the crystallization of this type occurs at shallow depths, while similar evolutionary trends in the compositions of rock-forming minerals for different-aged basalts of the northern and the southern sector indicate their genetic affinity and an affiliation with typical island arc formations. Taking into account these contradictions, viz., the island arc character of the magmas and the intraplate spinel type, one is led to suggest a relict nature for the high-alumina spinels from the KVC northern sector basalts. They may well reflect the composition of protocrystalline phases and melts during the earlier phases of magma generation in the KVC area occurring in a geodynamic mode that was different from the island arc type.

Another important factor to facilitate the crystallization of high-alumina spinel may have been the higher alumina content of the melt. Kamenetsky et al. [27] found the dependence of alumina content in spinels on that of the melt based on results of experimental studies, in particular, with melt inclusions. Low-titanium spinels containing 30–40% alumina can accordingly crystallize from primitive melts of Al_2O_3 content within 14–17%. The high alumina content for the basalts of the Malyi Semyachik volcanic center was discovered earlier [2, 18]. Selyangin [18] found an "anorthosite tendency" for the magma evolution in the Malyi Semyachik volcanic center. It should be noted that in this particular case, the high alumina content of primary melts in the KVC northern sector is also attested to by the composition of daughter crystalline phases in partially crystallized melt inclusions in olivines. These are represented by high-alumina phases, viz., fassaite and spinel (pleonaste) containing as much as 55% Al_2O_3. Such inclusions in olivines from the southern sector basalts also contain fassaite, but the spinellide have an intermediate composition with more iron.

Partially crystallized inclusions with daughter phases of fassaite and high-alumina spinel were also detected in olivines with $Mg^{\#}$ 86–91 from avachites (high-magnesia rocks in the Avacha Volcano edifice) [16].

It is a remarkable fact that fassaite and high-alumina spinel, which are regarded as rock-forming minerals, crystallize in the Cretaceous intraplate alkali basalts on Cape Kamchatskii [17], as well as in the Late Miocene alkali basalts of the Valaginskii Range [5]. The Valaginskii Range structure is west of Stena and Malyi Semyachik volcanoes. It should be noted that the basaltoids of increased alkalinity and titanium content that structure contains were found in the Pliocene basement of

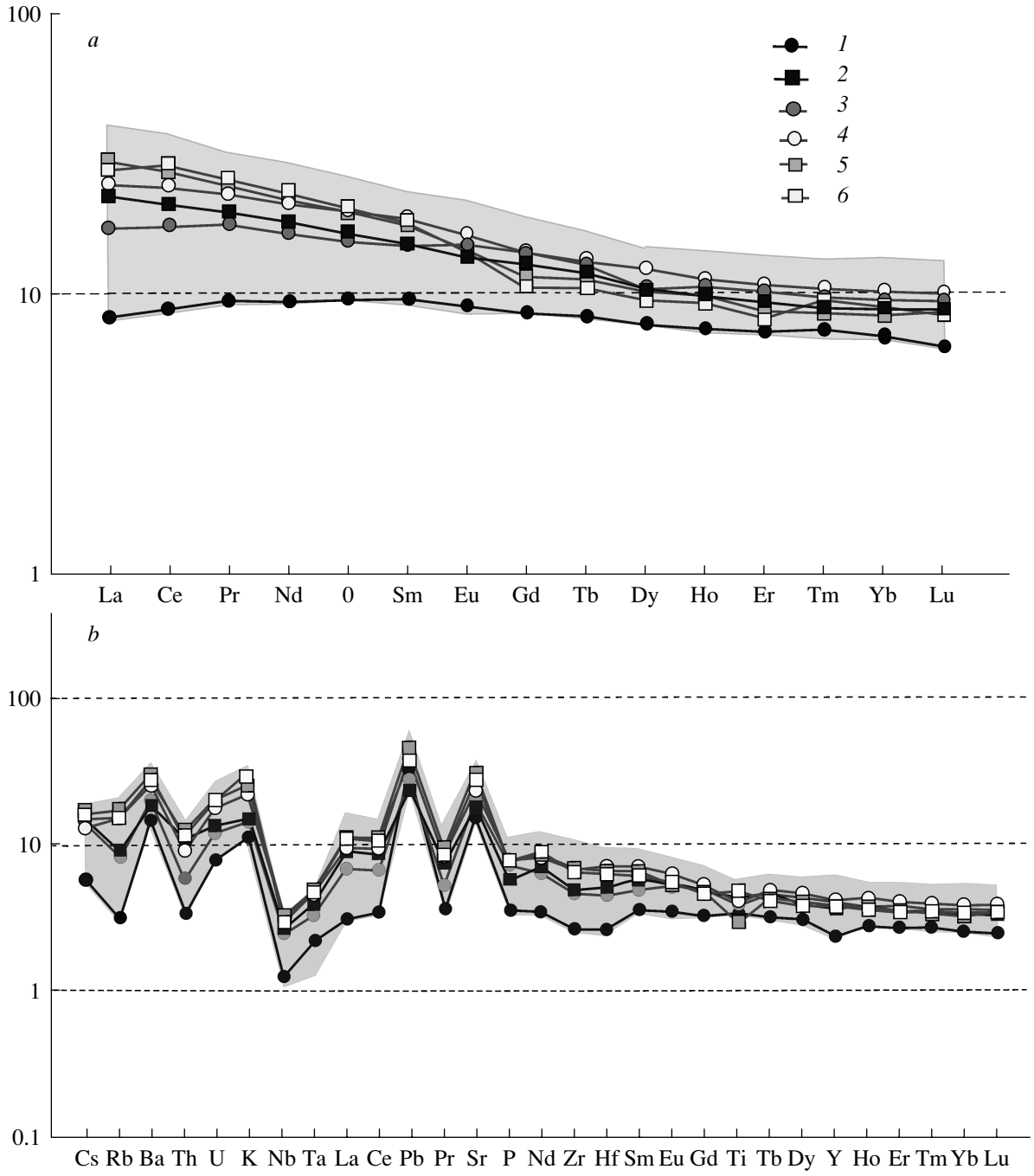

Fig. 8. Geochemistry of rare and rare-earth elements in olivine basalts of the Karymskii Volcanic Center: (*a*) distribution spectra of rare-earth elements normalized by chondrite, (*b*) spider diagrams of hygromagmatophile elements normalized by the primitive mantle. (*1–2*) pre-caldera volcanoes (*1* Stena, *2* Ditmara), (*3–4*) Upper Pleistocene/Holocene formations (*3* Malyi Semyachik Volcano, (*4*) dike in the northwest wall of the Karymskii caldera, (*5*) 4800 tephra, (*6*) 1996 tephra. The shaded field is the composition spectrum for basalts of the Karymskii Volcanic Center, including pyroxene varieties, (*c*) Th/Yb vs. Ta/Yb ratio diagram [29] for olivine basalts of the Karymskii Volcanic Center. The legend for figurative points is given in Fig. 7. Fields: light gray denotes basalts in the northern part of the Eastern volcanic belt of Kamchatka and the Central Kamchatka depression after [22], gray marks basalts of the Sredinnyi Range, ibidem.

the central part of the Eastern volcanic belt of Kamchatka, in particular, in the Uzon–Geyser volcano-tectonic depression [8] and in the Karymskii Volcanic Center (Mount Stol) [6]. The Al–Cr–Fe^{+3} diagram (Fig. 5a) shows aluminiferous spinels (two analyses) in olivines Fo 83–85 from basalts in the lower section of the Shchapina suite to be compositionally similar to 2 solid-phase spinel inclusions in olivine Fo 85 from

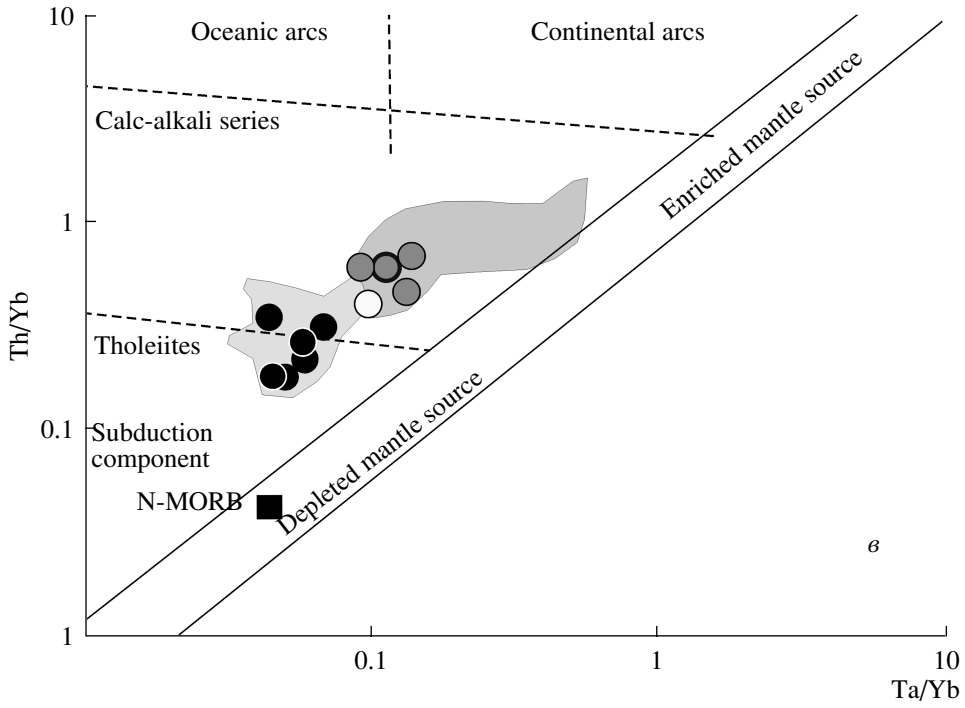

Fig. 8. Contd.

basalts of the Stena pre-caldera volcano [18]. Note that the composition of fassaite phenocrysts from the Shchapina basalts is mostly different from fassaite (the daughter phases) in melt inclusions found in the olivine of the basalts studied here (Table 5) in having a higher titanium content [5].

O.N. Volynets et al. [5] found that Late Miocene intraplate alkali basalts (the Shchapina suite) occur rather widely in eastern Kamchatka, while their geochemical characteristics change over time. For example, basalts in the upper section of the Shchapina suite occur in the field of marginal continental rift basalts, while the Upper Pliocene/Quaternary volcanites in the Eastern volcanic belt proper (the pre-caldera phase in the KVC evolution) possess typical island-arc geochemical features. An analysis of geochemical data [5] suggests a change in geodynamic mode during the evolution of the Eastern volcanic belt with accompanying changes in the conditions of magma generation and magma source depth, as well as with successive shifting of magma generation sources from deeper to shallower levels. In this connection the olivines and anorthites in the basalts of the northern sector of the Karymskii Volcanic Center that contain solid-phase inclusions of high-alumina spinel may be crystalline phases of magmas coming from intermediate crustal magma chambers during the preceding phase of alkali magmatism eruptions. The spatial proximity between the area of alkali basalts (the upper reaches of the Levaya Zhupanova River) and the primitive basalts of the pre-caldera Stena volcano, as well as their closely-spaced (on the scale of geological time) occurrence imply that a melt of the island-arc geochemical type may have captured material pertinent to the protocrystallization phase of alkali-basaltic magma of Miocene/Pliocene chambers during eruptions. In recent years studies in melt inclusions in basaltic minerals of the Eastern volcanic belt (including the Karymskii Volcanic Center) revealed alkali (nepheline-normative) melts with increased concentrations of sodium and titanium [15, 16, 19]. In this connection the occurrence of high-alumina minerals in melt inclusions in olivines (and anorthites) of the Karymskii Volcanic Center, which are typical of alkali melts, corroborate the idea that K–Na alkali magma melts were generated during the earlier phases in the evolution of the Eastern volcanic belt. It should be noted that the existence of "closer genetic relationships" between intraplate and island arc volcanites is, in contrast to earlier notions, hypothesized on the basis of mineralogical and geochemical investigations of ultrabasic inclusions in volcanites [12, 13].

An analysis of the deformations that preceded the 1996 explosive subaerial eruption of basaltic tephra on the north shore of Lake Karymskii (the Akademii Nauk caldera) gave a depth of the center of gravity of a magma chamber of 18 km [20]. Similarities in the mineralogic features for different-aged basalts of the Karymskii Volcanic Center suggest a common intermediate chamber of basaltic magma at a depth of 15–20 km (5–6 kbars) in the area, which has been periodically supplying high temperature melts to the surface from the Late Pliocene/Lower Pleistocene until the present time.

The wide range of dark minerals in the basalts of the southern sector of the Karymskii Volcanic Center indicates that at the time of eruption these were a disequilibrium mixture of a melt and mineral phases crystallizing at different depths. The KVC mineral associations contain high-chrome spinel, high-magnesia olivine and clinopyroxene, thus indicating a relationship of the common intermediate chamber to deeper magma generating zones, probably at the boundary of the lower crust and upper mantle. Judging from experimental data, the high-magnesia association of olivine and clinopyroxene might have crystallized at a pressure of 8–9 kbars (a depth of about 30 km) and temperatures greater than 1200°C [1]. During Upper Pleistocene/Holocene time (and in 1996), deep melts were ascending along a north–south fault in the southern sector of the Karymskii Volcanic Center and have been identified on the north shore of Lake Karymskii [9, 10, 14].

No relationship to lower crustal magma chambers has been identified by petrologic methods for the Stena and Malyi Semyachik basalts. Even though high-alumina spinel (a barophile mineral) has been detected both in pre-caldera basalts and Holocene basalts, the activity of Miocene/Pliocene magma-conducting zones is not very likely. At the same time, the low magnesia content of olivine and clinopyroxene and the gabbroid associations of phenocrysts in basalts, as well as the presence of holocrystalline gabbroid inclusions in lavas [18], all suggest a shallow (2–6 kbars) depth for their generation region. It is possible that such a long period of activity of volcanoes in the northern sector (of the order of 2–3 million years, including the Holocene) and a periodic supply of magnesia-rich Pl–Ol–Cpx basalts [18] may indicate some special tectonic environments occurring in that zone and providing a higher rate of basalt ascent from the intermediate magma chamber.

CONCLUSIONS

(1) The olivine basalts of the Karymskii Volcanic Center are typical low- and moderate-potassium tholeiite basalts of the island arc geochemical type characteristic for the Eastern volcanic belt of Kamchatka.

(2) The petrology of different-aged olivine basalts of the Karymskii Volcanic Center implies the existence of an intermediate chamber of basaltic magma at a depth of 15–20 km (5–6 kbars) where crystallization differentiation is taking place. From the Lower Pleistocene until today, the activity of that chamber controls a periodic supply of high-temperature basaltic melts to the surface.

(3) The geochemical features of the KVC basalts imply melt generation in a common depleted mantle source similar to N–MORB by successive crystallization of primary melts. As the basaltic melts were evolving, they were undergoing partial mixture with magma components crystallizing at different depths, and mineral cumulus associations were being assimilated.

(4) High-alumina spinel (hercynite) was identified as solid-phase inclusions in olivine (and anorthite) from basalts of the northern sector of the Karymskii Volcanic Center. We hypothesize a relict origin of the high-alumina spinel or its crystallization from high-alumina melts.

ACKNOWLEDGMENTS

The authors thank Dr. Sci. (Geol.–Mineral.) A.V. Koloskov for a constructive discussion of the paper, which helped improve it, M.Yu. Puzankov for aid in the use of geothermometers, V.M. Chubarov and T.M. Filosofova for qualitative microlog analysis, A.R. Dunin-Barkovskaya for help in treatment of graphic materials. We are grateful to Cand. Sci. (Geol.–Mineral.) V.L. Leonov and O.B. Selyangin for basalt specimens they lent for analysis.

The work was financially supported by the Russian Foundation for Basic Research, projects 05-05-64-730, 07-05-00-959, and 08-05-00-453, and by the Far East Division, Russ. Acad. Sci. project 06-III-A-08-329.

REFERENCES

1. Ariskin, A.A. and Barmina, G.S., *Modelirovanie fazovykh ravnovesii pri kristallizatsii bazal'tovykh magm* (Simulating Phase Equilibria during the Crystallization of Basaltic Magmas), Moscow: Nauka, 2000.
2. Babanskii, A.D., Ryabchikov, I.D., and Bogatikov, O.A., *Evolyutsiya shchelochno-zemel'nykh magm* (The Evolution of Alkaline-Earth Magmas), Moscow: Nauka, 1983.
3. Balashov, Yu.A., *Geokhimiya redkozemel'nykh elementov* (The Geochemistry of Rare Earths), Moscow; Nauka, 1976.
4. Belousov, A.B., Belousova, M.G., and Murav'ev, Ya.D., Holocene Eruptions in the Akademii Nauk Caldera and the Age of Karymskii Stratovolcano, Kamchatka, *Dokl. RAN*, 1997, vol. 354, no. 5, pp. 648–652.
5. Volynets, O.N., Uspenskii, V.S., Anoshin, G.N., et al., The Evolution of the Geodynamic Magma Generation in Eastern Kamchatka during Late Cenozoic Time: Geochemical Evidence, *Vulkanol. Seismol.*, 1990, no. 5, pp. 14–28.
6. *Vulkanicheskii tsentr: stroenie, dinamika, veshchestvo (Karymskaya struktura)* (The Structure, Dynamics, and Material of a Volcanic Center: The Karymskii Structure), Masurenkov, Yu.P., Ed., Moscow: Nauka, 1980.
7. Grib, E.N., The Petrology of Ejecta Discharged by the January 2–3 Eruption in the Akademii Nauk Caldera, *Vulkanol. Seismol.*, 1997, no. 5, pp. 71–97.
8. Grib, E.N., Perepelov, A.B., and Leonov, V.L., The Geochemistry of Volcanic Rocks in the Uzon–Geyser Depression, Kamchatka, *Vulkanol. Seismol.*, 2003, no. 4, pp. 11–28.
9. Grib, E.N. and Leonov, V.L., The Evolution of Magma Chambers beneath Calderas in the Southern Sector of the Karymskii Volcanic Center. Part I. Geology, Structure, and Composition of Pyroclastic Flows, *Vulkanol. Seismol.*, 2004, no. 4, pp. 21–40.
10. Grib, E.N. and Leonov, V.L., The Evolution of Magma Chambers beneath Calderas in the Southern Sector of the

Karymskii Volcanic Center. Part II. The PTF Conditions for the Crystallization of Ignimbrite-Forming Melts and the Evolution of the Magmatism, *Vulkanol. Seismol.*, 2004, no. 5, pp. 23–37.

11. Ivanov, B.V., *Izverzhenie Karymskogo vulkana v 1962-1965 g.g. i vulkany Karymskoi gruppy* (The 1962–1965 Eruption of Karymskii Volcano and the Volcanoes of the Karymskii Group), Moscow: Nauka, 1970.
12. Koloskov, A.V., Puzankov, M.Yu., and Pirozhkova, E.S., Ultramafic Inclusions in Island Arc Basaltoids: The Problem of the Composition and Genesis of the Transitional "Crust–Mantle Mixture" Layer in Island Arc Systems, in *Geodinamika i vulkanizm Kurilo-Kamchatskoi ostrovoduzhnoi sistemy* (The Geodynamics and Volcanism of the Kuril–Kamchatka Island Arc System), Petropavlovsk-Kamchatskii: IVGiG DVO RAN, 2001, pp. 123–152.
13. Koloskov, A.V., The Isotope Geochemical Inhomogeneity of Kamchatka Pliocene/Quaternary Volcanites, the Subduction Zone Geometry, a Model of the Fluid–Magma System, *Vulkanol. Seismol.*, 2001, no. 6, pp. 16–42.
14. Leonov, V.L. and Grib, E.N., *Strukturnye pozitsii i vulkanizm chetvertichnykh kal'der Kamchatki* (The Structural Settings and Volcanism of Quaternary Calderas in Kamchatka), Vladivostok: Dal'nauka, 2004.
15. Naumov, V.B., Tolstykh, M.L., Grib, E.N., et al., The Chemical Composition, Volatiles, and Admixture Elements in the Melts of the Karymskii Volcanic Center, Kamchatka and Golovnina Volcano, Kunashir I. from Studies of Inclusions in Minerals, *Petrologiya,* 2007, vol. 15, no. 6, pp. 563–581.
16. Portnyagin, M.V., Mironov, N.L., Matveev, S.V., et al., The Petrology of "Avachites"—High-Magnesia Basalts of Avacha Volcano, Kamchatka. Part II. Melt Inclusions in Olivine, *Petrologiya*, 2005, vol. 13, no. 4, pp. 358–388.
17. Savel'ev, D.P. and Filosofova, T.M., The Mineralogic Features of Cretaceous Alkali Basalts in the Kamchatskii Mys Peninsula, Eastern Kamchatka, *Vestnik KRAUNTs. Ser. Nauki o Zemle*, 2005, no. 5, pp. 94–101.
18. Selyangin, O.B., *Petrogenezis bazal't-datsitovoi serii v svyazi s evolyutsiei vulkanostruktur* (The Petrogenesis of the Basalt–Dacite Series in Connection with the Evolution of Volcanic Structures), Moscow: Nauka, 1987.
19. Tolstykh, M.L., Naumov, V.B., Ozerov, A.Yu., et al., The Composition of Magmas Discharged by the 1996 Eruption in the Karymskii Volcanic Center, Kamchatka from Studies of Melt Inclusions, *Geokhimiya*, 2001, no. 5, pp. 498–509.
20. Fedotov, S.A., On the Eruptions in the Akademii Nauk Caldera and on Karymskii Volcano, Kamchatka in 1996, the Study and Mechanism of These, *Vulkanol. Seismol.*, 1997, no. 5, pp. 3–38.
21. Khubunaya, S.A., Bogoyavlenskii, S.O., Novgorodtseva, T.Yu., et al., Mineralogic Features of Magnesia Basalts as Reflecting Fractionation in the Magma Chamber of Klyuchevskoi Volcano, *Vulkanol. Seismol.*, 1993, no. 3, pp. 46–68.
22. Churikova, T.G., Dorendorf, F., and Verner, G., The Nature of Geochemical Zonality across the Trend of the Kuril–Kamchatka Island Arc, in *Geodinamika i vulkanizm Kurilo-Kamchatskoi ostrovoduzhnoi sistemy* (The Geodynamics and Volcanism of the Kuril–Kamchatka Island Arc System), Petropavlovsk-Kamchatskii: IVGiG DVO RAN, 2001, pp. 173–190.
23. Arai, S. Compositional Variation of Olivine-Chromian Spinel in Mg-Rich Magmas as a Guide to their Residual Spinel Peridotites, *J. Volcanol. Geotherm. Res.*, 1994, vol. 114, pp. 279–293.
24. Avers, J., Trace Element Modeling of Aqueous Fluid–Peridotite Interaction in the Mantle Wedge of Subduction Zones, *Contrib. Mineral. Petrol.,* 1998, vol. 132, pp. 390–404.
25. Ballhaus, C., Berry, R., and Green, D., High-Pressure Experimental Calibration of the Olivine–Orthopyroxene–Spinel Oxygen Geobarometer: Implications for the Oxidation State of the Upper Mantle, *Contrib. Mineral. Petrol.*, 1991, vol. 107, pp. 27–40.
26. Ford, C., Russel, D., Graven, J., and Fisk, M., Olivine–Liquid Equilibria: Temperature, Pressure and Composition Dependence of the Crystal: Liquid Cation Partition Coefficients for Mg, Fe^{+2}, Ca and Mn, *J. Petrol.*, 1983, vol. 24, pp. 256–265.
27. Kamenetsky, V., Crawford, A., and Meffre, S., Factors Controlling Chemistry of Magmatic Spinel: An Empirical Study of Associated Olivine, Cr-Spinel and Melt Inclusions from Primitive Rocks, *J. Petrol.*, 2001, vol. 42, no. 4, pp. 655–671.
28. Mercier, J., Single-Pyroxene Thermobarometry, *Tectonophysics*, 1980, vol. 70, pp. 1–37.
29. Pearce, J.A., Role of the Sub-Continental Lithosphere in Magma Genesis at Active Continental Margins, in *Continental Basalts and Mantle Xenoliths*, Hawkesworth, C.J. and Norry, M.J., Eds., papers prepared for a UK Volcanic Studies Group meeting at the University of Leicester, Nantwich: Shiva Publ., 1983, pp. 230–249.

SPELL: 1. Volcanites, 2. compositionally, 3. suprasubduction, 4. subalumochromopicotites